PROCEEDINGS A

royalsocietypublishing.org/journal/rspa

Research



Cite this article: Panagiotou1 E, Kauffman LH. 2020 Knot polynomials of open and closed curves. *Proc. R. Soc. A* **476**: 20200124. http://dx.doi.org/10.1098/rspa.2020.0124

Received: 24 February 2020 Accepted: 1 July 2020

Subject Areas:

topology, computational mathematics

Keywords:

open knots, links, Kauffman bracket polynomial, Jones polynomial, knotoids, linking number

Author for correspondence:

Eleni Panagiotou e-mail: eleni-panagiotou@utc.edu

Electronic supplementary material is available online at https://doi.org/10.6084/m9.figshare. c.5063420.

THE ROYAL SOCIETY

Knot polynomials of open and closed curves

Eleni Panagiotou¹ and Louis H. Kauffman^{2,3}

¹Department of Mathematics and SimCenter, University of Tennessee at Chattanooga, Chattanooga, TN 37403, USA

²Department of Mathematics, Statistics and Computer Science University of Illinois at Chicago, Chicago, IL 60607-7045, USA

³Department of Mechanics and Mathematics, Novosibirsk State University, Novosibirsk, Russia

EP, 0000-0002-1655-6447

In this manuscript, we introduce a method to measure entanglement of curves in 3-space that extends the notion of knot and link polynomials to open curves. We define the bracket polynomial of curves in 3-space and show that it has real coefficients and is a continuous function of the curve coordinates. This is used to define the Jones polynomial in a way that it is applicable to both open and closed curves in 3-space. For open curves, the Jones polynomial has real coefficients and it is a continuous function of the curve coordinates and as the endpoints of the curve tend to coincide, the Jones polynomial of the open curve tends to that of the resulting knot. For closed curves, it is a topological invariant, as the classical Jones polynomial. We show how these measures attain a simpler expression for polygonal curves and provide a finite form for their computation in the case of polygonal curves of 3 and 4 edges.

1. Introduction

Open curves in space can entangle and even tie knots, a situation that arises in many physical systems of filaments, such as polymers, textiles, chemical compounds [1–6]. In different contexts, entanglement of filaments affects material properties, function or other aspects related to fluid mechanics, biology, chemistry or engineering [2,6,7]. To measure entanglement of open curves, it is natural to look for measures of complexity in the study of knots and links [8]. In applied knot theory, the term 'chain' is often used to refer to a single curve in 3-space (usually a polygonal curve). This helps communicate the results to an interdisciplinary audience

where physical filaments are often referred to as 'chains' (for example, polymer chains). To avoid any confusion to readers who are not familiar with the term 'chain', we use the term 'curve(s)' throughout the manuscript with the appropriate specification (in 3-space, polygonal etc.) when needed. Even though many strong and refined measures of topological complexity for knots and links have been created in the last century, such as knot and link polynomials [9–14], the only one that is sensitive on the configurations of open curves is the Gauss linking integral (introduced in 1877) [15]. In this work, we define knot and link polynomials of *open curves in 3-space*. To do this, we combine ideas of the Gauss linking integral and the notion of knotoids (open curve *diagrams* [16–19]).

A knot is a simple closed curve in space. Similarly, a link is formed by many simple closed curves in space that do not intersect each other. Two knots or links are equivalent if one can be continuously deformed to the other without allowing cutting and pasting. A topological invariant is a function over the space of knots or links that is invariant under such deformations [9,13,14]. When dealing with open curves, the above notion of topological equivalence is not useful, since any mathematical open curve can be deformed to another without cutting and pasting. In fact, one does not need a measure of complexity of open curves that is invariant under deformations, but rather a measure that varies continuously in the space of configurations. Such a measure is the Gauss linking integral. For two closed curves, the Gauss linking integral is an integer topological invariant that measures the algebraic number of times one curve turns around the other. For two open curves, it is a real number that is a continuous function of its coordinates. The Gauss linking integral has been very useful in measuring entanglement in physical systems of open or closed filaments [3,20–24]. However, more refined measures of entanglement of one, two or more components, are needed. In this direction, several approximation efforts have appeared, aiming at mapping an open curve to a knot type, or a knotoid type [6,25,26].

In this manuscript, we introduce a new measure of entanglement of open curves in 3-space that is a well-defined function of its coordinates in 3-space that does not approximate an open curve by any particular closed curve or any particular projection of the open curve. Namely, we define the *bracket polynomial of open curves in 3-space*, a polynomial with real coefficients which is a continuous function of the coordinates of the curve. This is used to define the *Jones polynomial of open curves in 3-space*. The Jones polynomial of open three-dimensional curves is a continuous function of the curve coordinates and, as the endpoints of the curve tend to coincide, it tends to the Jones polynomial of the resulting knot, a topological invariant of the knot. In general, the Jones polynomial of open curves is independent of the parametrization of the curve, but it depends on the relative positions of the curve coordinates. We stress that this is the first well-defined new measure of entanglement of open curves that is a continuous measure of complexity of open curves since the Gauss linking integral and it is stronger than the Gauss linking integral.

An important reason why the Gauss linking integral has been very useful in applications is that a finite form for its computation exists that avoids numerical integration [27]. To this direction, in this manuscript, we also provide a finite form for the computation of the bracket and Jones polynomials in the case of a polygonal curve of 3 and 4 edges (open or closed). This is the base case upon which the general case of more edges will be studied in a sequel to this paper.

The manuscript is organized as follows: §2 discusses background information on measures of entanglement, §3 gives the definition and properties of the bracket polynomial of open curves in 3-space and uses the bracket polynomial of open curves to define the Jones polynomial of open curves. We stress that, even though in this manuscript we focus on single open curves, all the definitions and properties of those described in §3 apply to a collection of open curves. Appendix A provides a finite formula for the computation of the Jones polynomial of a polygonal curve of 4 edges. A finite formula for the computation of the bracket polynomial of a polygonal curve of 3 and 4 edges is obtained in the electronic supplementary material.

2. Measures of complexity of open curves and their projections

In this section, we provide background information that is necessary for the rest of the manuscript. More precisely, we discuss the Gauss linking integral, a measure of entanglement of both open and closed *curves in 3-space* and the bracket and Jones polynomial of knotoids, a measure of complexity of open knot *diagrams* (projections of open curves in 3-space).

(a) The Gauss linking integral

A measure of the degree to which curves interwind is the Gauss linking integral:

Definition 2.1 (Gauss Linking Number). The Gauss *Linking Number* of two disjoint (closed or open) oriented curves l_1 and l_2 , whose parametrizations are $\gamma_1(t)$, $\gamma_2(s)$, respectively, is defined as the following double integral over l_1 and l_2 [15]:

$$L(l_1, l_2) = \frac{1}{4\pi} \int_{[0,1]} \int_{[0,1]} \frac{(\dot{\gamma}_1(t), \dot{\gamma}_2(s), \gamma_1(t) - \gamma_2(s))}{\|\gamma_1(t) - \gamma_2(s)\|^3} dt ds,$$
(2.1)

where $(\dot{\gamma}_1(t), \dot{\gamma}_2(s), \gamma_1(t) - \gamma_2(s))$ is the scalar triple product of $\dot{\gamma}_1(t), \dot{\gamma}_2(s)$ and $\gamma_1(t) - \gamma_2(s)$.

For closed curves, the Gauss linking integral is equal to half the algebraic sum of inter-crossings in the projection of the two curves in any projection direction, it is an integer and a topological invariant of the link.

For open curves, the Gauss linking integral is equal to the average of half the algebraic sum of inter-crossings in the projection of the two curves over all possible projection directions. It is a real number and a continuous function of the curve coordinates.

(i) Finite form of the Gauss linking integral

Downloaded from https://royalsocietypublishing.org/ on 17 April 2021

In [27], a finite form for the Gauss linking integral of two edges was introduced, which gives a finite form for the Gauss linking integral over two polygonal curves.

Let E_n , R_m denote two polygonal curves of edges e_i , i = 1, ..., n, r_i , j = 1, ..., m, then

$$L(E_n, R_m) = \sum_{i=1}^{n} \sum_{j=1}^{m} L(e_i, r_j),$$
(2.2)

where $L(e_i, r_j)$ is the Gauss linking integral of two edges. Let e_i be the edge that connects the vertices p_i , p_{i+1} and r_j be the edge that connects the vertices p_j , p_{j+1} (see figure 1 for an illustrative example). In [27], it was shown that $L(e_i, r_j) = \frac{1}{4\pi} \operatorname{Area}(Q_{i,j})$, where Q_{ij} for i < j denotes the quadrangle defined by the faces of the quadrilateral formed by the vertices p_i , p_{i+1} , p_j , p_{j+1} . This area can be computed by adding the dihedral angles of this quadrilateral. The faces of this quadrangle have normal vectors p_i , $i = 1, \ldots, 4$, defined as follows [28]:

$$n_1 = \frac{r_{i,j} \times r_{i,j+1}}{\|r_{ij} \times r_{i,j+1}\|}, \quad n_2 = \frac{r_{i,j+1} \times r_{i+1,j+1}}{\|r_{i,j+1} \times r_{i+1,j+1}\|}, \quad n_3 = \frac{r_{i+1,j+1} \times r_{i+1,j}}{\|r_{i+1,j+1} \times r_{i+1,j}\|}, \quad n_4 = \frac{r_{i+1,j} \times r_{i,j}}{\|r_{i+1,j} \times r_{i,j}\|},$$

where $r_{ij} = p_i - p_j$, $r_{i,j+1} = p_i - p_{j+1}$, $r_{i+1,j} = p_{i+1} - p_j$ and $r_{i+1,j+1} = p_{i+1} - p_{j+1}$.

The area of the quadrangle Q_{ij} is: Area (Q_{ij}) = arcsin $(n_1 \cdot n_2)$ + arcsin $(n_2 \cdot n_3)$ + arcsin $(n_3 \cdot n_4)$ + arcsin $(n_4 \cdot n_1)$.

(b) The bracket polynomial of knotoids

The theory of knotoids was introduced by V.Turaev [19] in 2012 (see also [16]). Knotoids are open-ended knot diagrams (figure 2). Three *Reidemeister moves* (figure 3*a*), are defined on knotoid diagrams by modifying the diagram within small surrounding discs that do not use the endpoints (forbidden moves shown in figure 3*b*). Two knotoid diagrams are said to be equivalent if they are related to each other by a finite sequence of such moves (and isotopy of S^2 , R^2 for knotoid diagrams in S^2 , R^2 , respectively).

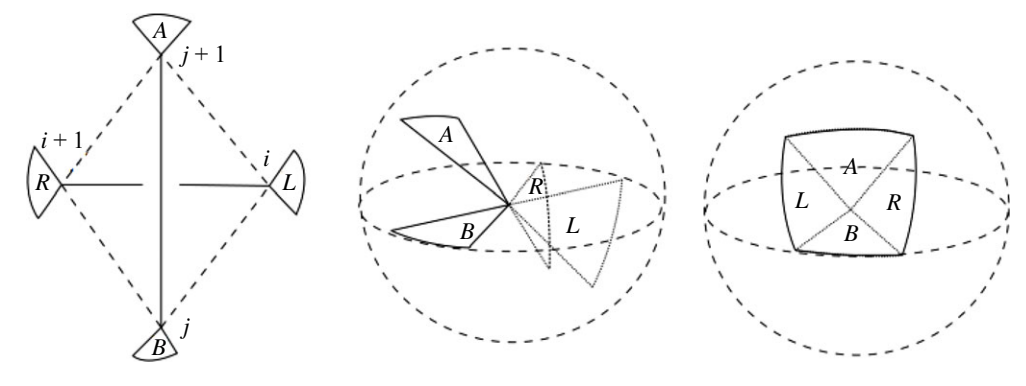




Figure 2. Examples of (polygonal) knotoids (open simple arc diagrams). Note that knotoids refer to *projections of open curves*, while knots refer to closed curves in 3-space.

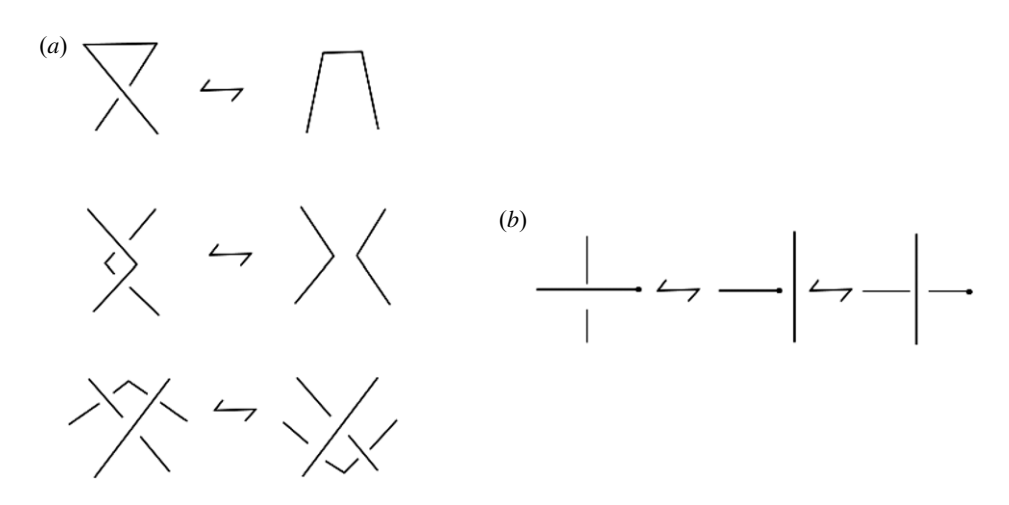


Figure 3. (a) The Reidemeister moves for knotoids and (b) forbidden knotoid moves.

The bracket polynomial of knotoids in S^2 or R^2 is defined by extending the state expansion of the bracket polynomial of knots. The following initial conditions and diagrammatic equations are sufficient for the skein computation of the bracket polynomial of classical knotoids:

$$\langle \rangle \rangle = A \langle \rangle \rangle + A^{-1} \langle \rangle \langle \rangle, \quad \langle K \cup \bigcirc \rangle = (-A^2 - A^{-2}) \langle K \rangle, \quad \langle \bullet \bullet \rangle = 1. \tag{2.3}$$

Definition 2.2. A state of a diagram of a knotoid, *K*, consists in a choice of local state for each crossing of *K*.

Definition 2.3. The bracket polynomial of a knotoid diagram *K* is defined as

$$\langle K \rangle = \sum_{S} A^{\sigma(S)} d^{\|S\| - 1}, \tag{2.4}$$

where the sum is taken over all states, $\sigma(S)$ is the sum of the labels of the state S, ||S|| is the number of components of S, and $d = (-A^2 - A^{-2})$.

Remark 2.4. The classical bracket polynomial of knots is defined using formula (2.4), with the same Skein relations as in equation (2.3), except the last one, where an arc is replaced by a circle. The classical bracket polynomial is not a topological invariant for knots (it is not invariant under the Reidemeister 1 move) and depends on the knot diagram used for its computation. Similarly, the bracket polynomial of knotoids is not invariant under Ω_1 (the Reidemeister 1 move) and depends on the knotoid diagram.

(i) The Jones polynomial of knotoids

The Jones polynomial of knotoids is an invariant of knotoids and many component knotoids, called multiknotoids or linkoids, (equivalent knotoids/linkoids map to the same polynomial) and can be defined using the normalized bracket polynomial. The normalized bracket polynomial is defined as follows:

$$f_K = (-A^{-3})^{-wr(K)} \langle K \rangle, \tag{2.5}$$

where wr(K) is the writhe of the knotoid diagram K.

The normalized bracket polynomial of knotoids in S^2 generalizes the Jones polynomial of knotoids with the substitution $A = t^{-1/4}$.

Remark 2.5. The same definition, where *K* is a knot diagram, applies to simple closed curves to give the Jones polynomial of knots and links, a topological invariant of knots and links.

3. The bracket polynomial of a curve in 3-space

Consider an open or closed curve in 3-space. A (regular) projection of a curve (fixed in 3-space) can give a different knotoid diagram (or knot diagram), depending on the choice of projection direction. We define the bracket polynomial of a curve in 3-space as the *average* of the Kauffman bracket polynomial of a projection of the curve over all possible projection directions. The definition is made precise as follows:

Definition 3.1. Let l denote a curve in 3-space. Let $(l)_{\xi}$ denote the projection of l on a plane with normal vector ξ . The bracket polynomial of l is defined as

$$\langle l \rangle = \frac{1}{4\pi} \int_{\xi \in S^2} \langle K((l)_{\xi}) \rangle \, \mathrm{d}S, \tag{3.1}$$

where the integral is over all vectors in S^2 except a set of measure zero (corresponding to irregular projections, i.e. projections where more than two points coincide).

Properties of the bracket polynomial of curves in 3-space

corollary 3.4).

- (i) The bracket polynomial defined in equation (3.1) does not depend on any particular projection of the curve (open or closed).
- (ii) For an open curve this polynomial is not the polynomial of a corresponding/approximating closed curve, nor that of a corresponding/approximating knotoid.
- (iii) For both open and closed curves, the bracket polynomial defined in equation (3.1) has real coefficients.
- (iv) The bracket polynomial defined in equation (3.1) is not a topological invariant, but it is a continuous function of the curve coordinates for both open and closed curves (see

In the following, we will show that the bracket polynomial of curves in 3-space attains a simpler expression for polygonal curves. However, similar arguments can be used to extend this simpler expression to any curve in 3-space (polygonal or not).

Let EW_n denote the space of configurations of polygonal curves of n edges. Let E_n denote a polygonal curve of n edges in 3-space. Then only a finite number of different knotoid (or knot) types can occur in any projection of E_n . Let k(n) be the total number of knotoids that can be realized by a projection of a three-dimensional polygonal curve with n edges, we denote K_i , $i = 1, \ldots, k(n)$.

Then equation (3.1) is equivalent to the following sum:

$$\langle E_n \rangle = \sum_{i=1}^k p_i^{(n)} \langle K_i \rangle, \tag{3.2}$$

where $K((E_n)_{\xi})$ denotes the knotoid corresponding to $(E_n)_{\xi}$ and we denote $p_i^{(n)}$, the probability that a projection of E_n gives knotoid K_i , i.e. $p_i^{(n)} = P(K(E_n)_{\xi} = K_i)$.

Let m denote the maximum degree of (K_i) , i = 1, ..., k and let L_m denote the space of Laurent polynomials of degree less than or equal to m. Then (E_n) is a function from EW_n to L_m .

Lemma 3.2. The probability $p_i^{(n)}$ is a continuous function of the coordinates of E_n .

Proof. Note that

$$p_i^{(n)} = \frac{2A_0}{4\pi},\tag{3.3}$$

where A_0 = area on the sphere corresponding to vectors ξ such that: $K((E_n)_{\xi}) = K_i$. For a polygonal curve, this area will be bounded by a finite number of great circles, each of which is determined by an edge and a vertex of the polygonal curve, as in [27].

Let $\epsilon > 0$. Let a_i be the position of a vertex of E_n . Let $d = \min_{k,l} d_{k,l}$, where $d_{k,l} = \operatorname{dist}(a_i, a_k - a_l)$ (the distance between the vertex a_i and the segment connecting a_k, a_l). Suppose that a_i changes by δa , such that $\|\delta a\| < 2\pi \ d\epsilon/8(n-2)$. Then, the projection of the edges $e_{j-1} = a_j - a_{j-1}$ and $e_j = a_j - a_{j-1}$ $a_{i+1} - a_i$ in any projection direction might change and the great circles involving the vertex a_i might change as well. Each of these two edges, e_{i-1} , e_i is involved in (n-2) pairs of edges with which they may cross in a projection and each such pair consists of 3 faces containing a_i , one of which is counted in both the e_{i-1} and the e_i pairs. Thus, a change in a_i can affect 4(n-2)planes. Let u be the normal vector to one of these planes, say the one formed by the vertices a_i , a_i , a_{i+1} . The normal vector to the new plane containing $a_i + \delta a$, a_i , a_{i+1} , will change to $u + \delta u$. If that plane was one of the great circles bounding A_0 , then A_0 may also change to A'_0 (and $p_i^{(n)}$ to $p_i^{\prime(n)}$, accordingly). The change in area $|A_0 - A_0'|$ will be bounded above by the area of the lune defined by the great circles with normal vectors u and $u + \delta u$, which is equal to $\alpha = 2\theta$, where θ is the dihedral angle between the two great circles, which is equal to the angle between u and $u + \delta u$. The maximum value of that angle will occur if δa is orthogonal to the plane a_i, a_l, a_{l+1} , which means when δa is parallel to u. Then the angle θ is that of a right triangle with one edge of length $d_{k,l} = dist(a_l, a_k - a_l)$ and the other of length $\|\delta a\|$. Thus $\tan \theta = \|\delta a\|/d_{k,l}$. Thus, the change in the area is

$$|A_0 - A_0'| \le 4(n-2)2\arctan\left(\frac{\|\delta a\|}{d}\right) < 8(n-2)\arctan\left(\frac{2\pi d\epsilon}{8(n-2)d}\right)$$

$$\approx 8(n-2)\frac{2\pi\epsilon}{8(n-2)} = 2\pi\epsilon,$$
(3.4)

where we used the small angle approximation. Thus $|p_i^{(n)} - p_i'^{(n)}| < \epsilon$.

Proposition 3.3. The bracket polynomial $\langle E_n \rangle = \sum_j q_j A^j$, is a continuous function of the curve coordinates. In other words, it is a continuous function in the space of configurations of E_n .

Proof. We consider the standard Euclidean norm over the space of Laurent polynomials of a fixed degree. Then $\|\langle E_n \rangle\| = \sqrt{\sum_j q_j^2}$. Since each coefficient q_j is a finite sum of probabilities of the form $p_i^{(n)}$, it is a continuous function of the curve coordinates. It follows that $\langle K(E_n) \rangle$ will also be continuous with the norm mentioned above.

Corollary 3.4. The bracket polynomial of a curve l in space, $\langle l \rangle$, is a continuous function in the space of configurations of l.

Proof. By approximating l by a polygonal curve, l_n and taking the limit as $n \to \infty$ by proposition 3.3, follows that l is continuous.

(a) The Jones polynomial of open curves in 3-space

The Jones polynomial of an open curve in 3-space is defined using the normalized bracket polynomial of an open curve. Even though we focus on open curves, the following definition applies also to closed curves, we therefore define it more generally for any curve in 3-space as follows:

Definition 3.5. Let l denote a curve in 3-space. Let $(l)_{\xi}$ denote the projection of l on a plane with normal vector ξ .

The normalized bracket polynomial of l is defined as

$$f_{K(l)} = \frac{1}{4\pi} \int_{\xi \in S^2} (-A^3)^{-wr((l)_{\xi})} \langle (l)_{\xi} \rangle \, dS, \tag{3.5}$$

where the integral is over all vectors in S^2 except a set of measure zero (corresponding to irregular projections).

Remark 3.6. The same definition applies to define the bracket and Jones polynomial of many open and/or closed curves in space by replacing l by a many component open/closed or mixed collection of open and closed curves. In the case of a collection of closed curves (a traditional link), the Jones polynomial is a topological invariant. In the case of open curves, it is a continuous function in the space of configurations. In this manuscript, we focus on one component, but the same analysis holds for many curves in 3-space.

Properties of the Jones polynomial of curves in 3-space

- (i) For closed curves, the Jones polynomial defined in equation (3.5) is a topological invariant and coincides with the classical Jones polynomial of a knot (see corollary 3.7).
- (ii) For open curves, the Jones polynomial has real coefficients and is a continuous function of the curve coordinates (see corollary 3.8).
- (iii) For an open curve the Jones polynomial is not the polynomial of a corresponding/approximating closed curve, nor that of a corresponding/approximating knotoid.

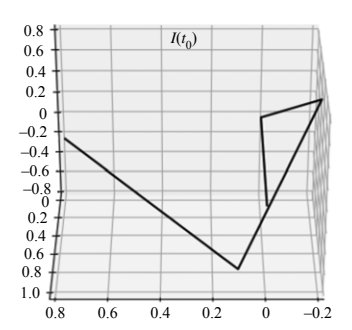
Corollary 3.7. In the case where l is a closed curve, $f_l = (-A^3)^{-wr((l)_{\xi})} \langle (l)_{\xi} \rangle$ for all $\xi \in S^2$.

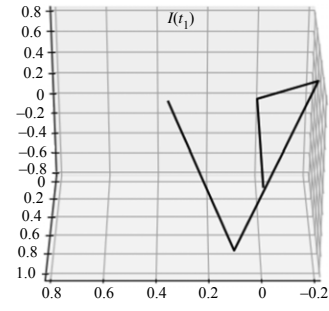
Proof. Let l be a closed curve, and let $\xi \in S^2$. Then its projection l_{ξ} is a knot diagram and $(-A^3)^{-wr((l)_{\xi})}\langle (l)_{\xi}$ is a topological invariant that does not depend on the particular diagram of the knot. Thus $f_l = (1/4\pi) \int_{\xi \in S^2} (-A^3)^{-wr((l)_{\xi})} \langle (l)_{\xi} \rangle \, \mathrm{d}S = (1/4\pi) 4\pi (-A^3)^{-wr((l)_{\xi})} \langle (l)_{\xi} \rangle$.

For a polygonal curve of n edges, equation (3.5) is equivalent to the following sum:

$$f_{(E_n)} = \sum_{i=1}^k \sum_{j=-m}^m p_{i,j}^{(n)} (-A^3)^{-j} \langle K_{i,j} \rangle, \tag{3.6}$$

where we denote $p_{i,j}^{(n)} = P(K(E_n)_{\xi} = K_i, wr((E_n)_{\xi}) = j), k = k(n) \text{ and } m = m(n, i).$





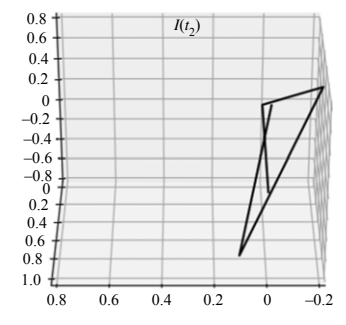


Figure 4. Three snapshots of a polygonal curve in 3-space with 3 fixed edges and one deforming edge in 3-space. From t_0 to t_2 , the curve tightens a configuration that gives the knotoid k2.1 in most projection directions and could lead to the creation of a trefoil knot if was able to thread through (more edges are needed for that [29]).

Corollary 3.8. The normalized bracket polynomial of an open curve in 3-space is a continuous function of the curve coordinates.

Proof. In a similar way as in lemma 3.2, one can show that for a polygonal curve of n edges, $p_{i,j}^{(n)}$ is a continuous function of the curve coordinates for all i, j, n and use that for the limiting case of any simple curve l in 3-space.

Example. In this example, we compute the Jones polynomial of an open polygonal curve in 3-space. We focus on the case of a curve with 4 edges, but this method applies to curves of any length. In appendix A, we derive an exact finite formula for equation (3.6) which avoids integration and is used in this example.

Figure 4 shows three snapshots of a polygonal curve, I, whose last edge deforms with time as the last vertex position changes according to the parametrization $I(t) = ((0,1,0), (0,0,0), (-0.2,0.8,0.8), (0.1,0.8,-0.8), (0.1+1.2\cos(a+t),0.5,-0.8+1.2\sin(a+t)))$. Therefore, for each value of the parameter t, we obtain a different curve in 3-space which differs from the first only in the position of its last vertex. The coordinates of the curve in the three snapshots in figure 4 are obtained for $t_0 = 0$, $t_1 = 4000$ and $t_2 = 11\,300$, in units of $2\pi/100\,000$, and $a = 32\,000\pi/100\,000$.

The Kauffman bracket at the start and end time is

$$\langle I(t_0) \rangle = 0.06A^2 - 0.77A^{-3} - 0.06A^{-4} + 0.07A^{-6} + 0.15$$

 $\langle I(t_2) \rangle = 0.71A^2 - 0.71A^{-4} - 0.14A^{-3} + 0.05A^{-6} + 0.14$

$$(3.7)$$

and

to be compared with the values of the bracket polynomial of the typical configuration of the right-handed trefoil knot, T_R and the right-handed k2.1 knotoid, which are equal to

$$\langle T_R \rangle = A^{-7} + A^5 - A^{-3}$$
 and $\langle k2.1 \rangle = A^2 - A^{-4} + 1$, respectively. (3.8)

The Jones polynomial at each time is

$$f(I(t_0)) = 0.06t - 0.06t^{5/2} + 0.06t^{3/2} + 0.94$$

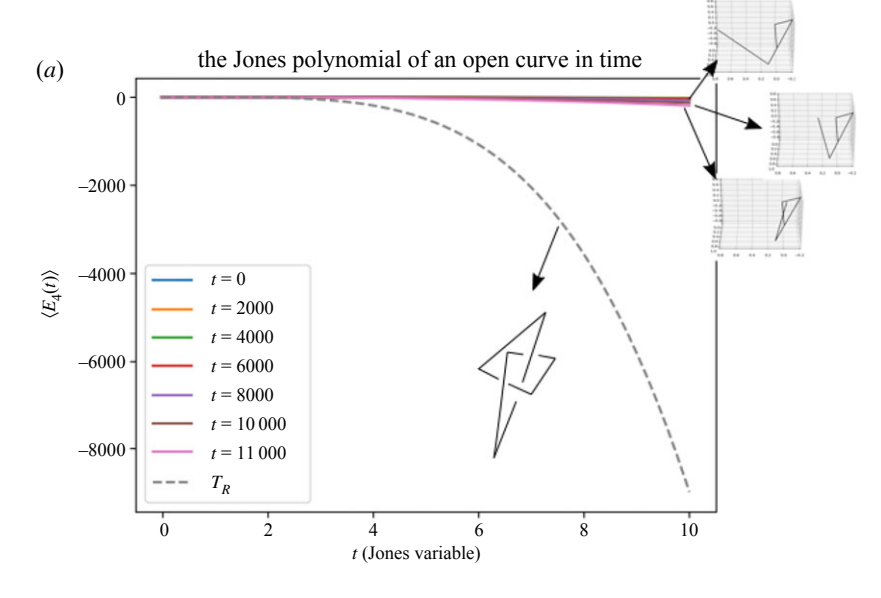
$$f(I(t_2)) = 0.71t - 0.71t^{5/2} + 0.71t^{3/2} + 0.29$$
 (3.9)

and

to be compared with the Jones polynomial of the right-handed trefoil knot, T_R and the right-handed k2.1 knotoid, which are equal to

$$f(T_R) = t + t^3 - t^4$$
 and $f(k2.1) = t + t^{3/2} - t^{5/2}$, respectively. (3.10)

Figure 5 shows the Jones polynomials at different times as the curve attains a more compact configuration as time increases. For comparison, the Jones polynomial of the trefoil knot (above) and of the two-dimensional knotoid diagram *k*2.1 (below) are shown as well. Note that a polygonal curve needs at least 6 edges to form a trefoil knot [29]. Nevertheless, in figure 5*a*, we



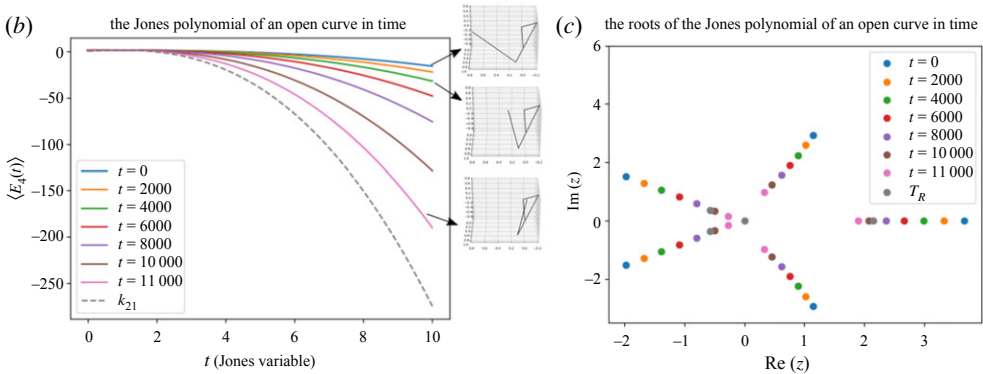


Figure 5. The Jones polynomial of the polygonal curve in 3-space as it deforms in time to tighten a compact configuration. (a) The dotted curve shows the Jones polynomial of the trefoil knot (we denote T_R). Even though a polygonal curve with 4 edges cannot form the trefoil knot [29], we see that the polynomial of the open curve tends to that of the trefoil knot, as this part of the configuration would be a part of the knotting pathway towards a trefoil knot. (b) The dotted curve shows the Jones polynomial of the knotoid k2.1 (a two-dimensional diagram). We see that the curve tightens to a configuration that in most projections will give the knotoid k2.1, which explains why the polynomials tend to that of k2.1. (c) The roots of the Jones polynomial of the open curve in 3-space as a function of time and the roots of the trefoil polynomial. (Online version in colour.)

see a small but continuous change of the polynomial closer to that of the trefoil knot. Indeed, we note that the tight configuration that attains the open curve in 3-space would be a necessary part of the knotting pathway of the open curve to form a trefoil knot. In figure 5*b*, we also plot the Jones polynomial of the open curve in 3-space as a function of time and the Jones polynomial of the knotoid diagram of k2.1. We see that the Jones polynomial of the open curve tends to that of the two-dimensional knotoid k2.1. Indeed, as the configuration tightens, it almost becomes two-dimensional, giving in most projections the knotoid k2.1. However, it will never be exactly equal to that. In figure 5*c*, we plot the roots of the Jones polynomial in time and those of the trefoil knot.

Remark 3.9. Using the state formula for the bracket polynomial of a knotoid, we obtain the following state formula for the bracket polynomial of a polygonal curve in 3-space

$$\langle E_n \rangle = \sum_{i=1}^k p_i^{(n)} \sum_{j=1}^{m_i} A^{\sigma(S_j)} d^{\|S_j\| - 1}, \tag{3.11}$$

royalsocietypublishing.org/journal/rspa Proc. R. Soc. A 476: 20200124

where the first sum is taken over all realizable knotoids of n edges and the second sum is taken over all states, S_i , of the *i*-th realizable knotoid, $\sigma(S_i)$ is the sum of the labels of the state S_i , $||S_i||$ is the number of components of S_i , and $d = (-A^2 - A^{-2})$.

Similarly, we obtain the following state formula for the normalized bracket polynomial of a polygonal curve in 3-space

$$f_{(E_n)} = \sum_{i=1}^k \sum_{j=1}^m p_{i,j}^{(n)} (-A^3)^{-j} \sum_{S_i} A^{\sigma(S_i)} d^{\|S_i\| - 1}.$$
 (3.12)

Remark 3.10 (Comparison with previous methods). Due to the urgency of measuring complexity in physical systems, several approaches have appeared in the last decade that attempt to use knot and link polynomials [6,16,26,30,31]. The underlying idea in these methods is to approximate an open curve in 3-space by a knot (dominant knot) or by a knotoid (dominant knotoid) that best captures its entanglement. Both the dominant knot and the dominant knotoid have been successful in characterizing proteins [6,26]. Even though these approaches are very helpful, they can at best approximate an open curve by either one closed curve or by one of its projections, respectively, and in practice, they might even give different answers for different choice of points on the sphere. Putting these methods in the framework, we established in this paper, they consist in computing the knot-type or the knotoid type with highest probability of occurring in a projection. In this study instead, we use the average of all the bracket polynomials of all the knotoids that occur. As we discussed in the previous paragraphs, this simple modification provides for the first time a well-defined measure of entanglement of open curves, other than the Gauss linking integral (see all the properties mentioned above). To understand the difference between the information captured by the two methods, we draw a comparison between the linking number and the Gauss linking integral: the dominant knot/knotoid method would correspond to the integer linking number that occurs in the most projections of an open curve, while the definition we give here, would correspond to that of the Gauss linking integral (the average linking number over all projections).

4. Conclusion

In this work, we defined the Kauffman bracket polynomial and the Jones polynomial in a way that is applicable to both open and closed curves in 3-space. We showed that for open curves these are continuous functions in the space of configurations. In doing this, we introduced a new method of measuring complexity of open curves, that combines the fundamental concepts of the Gauss linking integral and the theory of knotoids. This approach opens a new direction of research in applied knot theory where the machinery of knot and link polynomials can be rigorously applied to open curves for the first time.

Moreover, we showed how these functions of complexity obtain a finite form for polygonal curves. We derived specific finite formulae for the computation of the Jones polynomial in the basic case of a polygonal curve of 4 edges. This study lays the foundation for the derivation of a finite form for a larger number of edges. We stress that the number of edges that are relevant in applications, such as polymers, may not be equal to the exact number of covalent bonds, but rather equal to the number of Kuhn segments or equal to the number of entanglement strands in a primitive path [23,32,33], for which, even less than 10 edges are relevant. Similarly, proteins may be represented by their sequence of secondary structure elements as building blocks, for which less than 10 edges may also be relevant [34].

Even for this small number of edges, our numerical results show that the polynomials are sensitive to the motion of the polygonal curve and indicative of the transition to more compact conformations. For a larger number of edges these measures will directly reflect the entanglement of the open curve and how knotting occurs. We stress that these tools can also be applied to collections of open and closed curves and we expect them to have impactful applications. They allow to be included in formulations of mechanical models of elastic coils [35,36]. Also, they allow to accurately describe knotting pathways in proteins for the first time [37]. As well as in theories that derive important quantities in polymer physics, such as the entanglement length [4,22,23].

Data accessibility. The numerical results presented in the manuscript are obtained through application of the formulae described in the manuscript for the particular example whose details are also given in the manuscript. Therefore, all the numerical results presented in our manuscript are fully reproducible given the information in the manuscript. Similarly, all the numerical results presented in the electronic supplementary material of our manuscript are fully reproducible given the information in the manuscript and in the electronic supplementary material.

Authors' contributions. Both authors made substantial contributions to conception and design; drafting the article or revising it critically for important intellectual content; gave final approval of the version to be published; and gave agreement to be accountable for all aspects of the work in ensuring that questions related to the accuracy or integrity of any part of the work are appropriately investigated and resolved.

Competing interests. We declare we have no competing interest.

Funding. E.P. was supported by NSF (grant no. DMS-1913180). L.H.K. was supported by the Laboratory of Topology and Dynamics, Novosibirsk State University (contract no. 14.Y26.31.0025 with the Ministry of Education and Science of the Russian Federation).

Appendix A. A finite form for the Jones polynomial of an open polygonal curve with 4 edges

In this section, we show that an equivalent finite form of the normalized bracket polynomial (Jones polynomial) exists, reducing the computation of the integral to a computation of a few dot and cross products between vectors and some arcsin evaluations. Here, we provide a finite form of the normalized bracket polynomial for a polygonal curve of 4 edges. This could lead to the creation of its finite form for more edges.

Note that the case of closed curves is reduced to the Jones polynomial of any projection of the closed curve. Thus, here we focus on the open case where the average over all projections is needed. In the case of a polygonal curve with 3 edges, we denote E_3 , the Jones polynomial is always trivial.

Let E_4 be composed by 4 edges, $e_1, e_2.e_3, e_4$, connecting the vertices (0, 1), (1, 2), (2, 3), (3, 4), respectively.

Proposition A.1. k(4) = 2 (There are only two different knotoids that can be realized by a three-dimensional polygonal curve with 4 edges).

Proof. In a projection of E_4 , crossings may occur only between the projections of the pairs of edges: e_1 , e_3 , e_1 , e_4 and e_2 , e_4 . Therefore, we have the following five possible combinations (figure 6):

case A: one crossing, between the projections of: e_1 , e_3 or e_1 , e_4 or e_2 , e_4

case B: two crossings, between the projections of: e_1 , e_3 and e_1 , e_4 (giving two possible diagrams, i and i') or e_2 , e_4 and e_1 , e_4 (giving two possible diagrams, ii and ii') or e_1 , e_3 and e_2 , e_4 (not realizable, see below)

case C: three crossings, between the projections of: e_1 , e_3 and e_1 , e_4 and e_2 , e_4 .

The case B with e_1 , e_3 and e_2 , e_4 crossings is not realizable: The projection of e_1 defines a line in the plane that divides it in two regions. Suppose that the projection of e_3 intersects e_1 . Then the endpoints of e_3 lie in opposite regions and are the endpoint and the starting point of e_2 and e_4 , respectively. Thus the starting point of e_4 is in the opposite region of the one where e_2 lies in and to intersect e_2 it must also intersect e_1 .

respectively. Thus the starting point of e_4 is in the opposite region of the one where e_2 lies in and to intersect e_2 it must also intersect e_1 .

Figure 6 shows the different cases of diagrams with undefined over or under crossings which give rise to realizable knotoids. The diagrams of case A and case B (i') and (ii') are all trivial and

case C is realizable only when it is trivial. The diagrams of case B (i) and (ii) are non-trivial (in

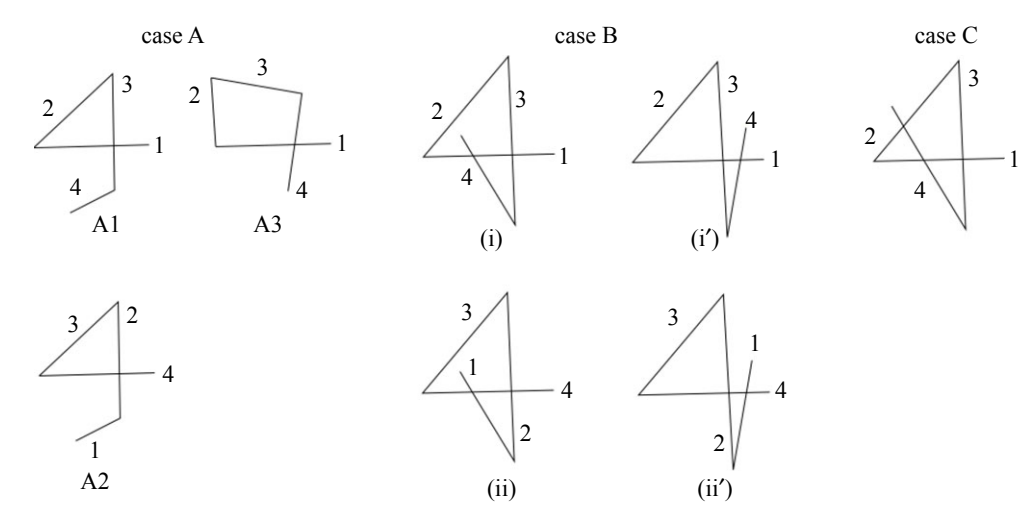


Figure 6. Possible diagrams of a projection of a polygonal curve with 4 edges, e_1 , e_2 , e_3 , e_4 . Each crossing may be over or under, except for case C, where constraints apply due to the polygonal curve rigidity (see proof of proposition A.1). Only case B (i) and (ii) can give a non-trivial knotoid when both crossings have the same sign. Therefore, if $(E_4)_{\xi}$ is non-trivial, it is of only one type: k2.1.

 S^2) only when the crossings between the involved edges have the same sign, i.e. $\epsilon_{1,3} = \epsilon_{1,4}$ or $\epsilon_{1,4} = \epsilon_{2,4}$, resp., in which case, they both represent the knotoid k2.1 [16].

The next proposition shows that when the projection of E_4 is of type k2.1, it can be only one of the two possible k2.1 diagrams (case B (i) or (ii)) in any projection direction.

Proposition A.2. Let E_4 denote a polygonal curve of 4 edges in 3 space. If there is ξ_1 such that $(E_4)_{\xi_1} =$ case B(i), then there does not exist $\xi \in S^2$, $\xi \neq \xi_1$ such that $(E_4)_{\xi} = B(ii)$ (and vice versa).

Proof. Without loss of generality, suppose that $\epsilon_{1,3} = \epsilon_{1,4} = 1$ and that there exists ξ_1 such that $(E_4)_{\xi_1}$ is of the form (i). Then, $(e_3 \times e_4) \cdot e_1 > 0$. Suppose that there is ξ_1 such that $(E_4)_{\xi_1}$ is of the form (ii). Then $(e_3 \times e_4) \cdot e_1 < 0$, contradiction.

Let E_4 denote a polygonal curve of 4 edges. Then, by propositions A.1 and A.2, the only non-trivial bracket polynomial is k2.1 and the writhe of the diagram is either 2 or -2. Thus the normalized bracket (Jones) polynomial of E_4 has the following form:

$$f(E_4) = p_{k2.1}^{(4)}((-A)^3)^{-(\pm 2)} \langle k2.1 \rangle + \sum_{j=-2}^{2} p_{k0,j}^{(4)} \cdot 1$$

= $p_{k2.1}^{(4)}((-A)^3)^{-(\pm 2)} \langle k2.1 \rangle + (1 - p_{k2.1}^{(4)}),$

where $p_{k2.1}^{(4)} = P(K((E_4)_{\xi}) = k2.1)$ and $p_{k0,j}^{(4)} = P(K((E_4)_{\xi}) = k0, wr((E_4)_{\xi}) = j)$.

Downloaded from https://royalsocietypublishing.org/ on 17 April 202

The rest of this section is focused on obtaining finite form for $p_{k2.1}^{(4)}$ (which is derived in theorem A.9).

In the following definition, we gather some of the notation used so far, together with some new definitions, necessary for the rest of the manuscript.

Definition A.3. Throughout this manuscript, we will denote by $Q_{i,j}$ the spherical polygon which corresponds to projections where the edges e_i, e_j cross. $Q_{i,j}^A$ is the antipodal of $Q_{i,j}$ on the sphere. $Q_{i,j,k}$ is the spherical polygon which corresponds to projections where the edges e_i, e_j and e_i, e_k cross, it is equal ro $Q_{i,j,k} = (Q_{i,j} \cap Q_{i,k}) \cup (Q_{i,j}^A \cap Q_{i,k})$. $Q_{i,j,k}^A$ is the antipodal of $Q_{i,j,k}$ on the sphere. We denote (w_1, \ldots, w_k) the spherical polygon formed by the intersection of great

royalsocietypublishing.org/journal/rspa Proc. R. Soc. A 476: 20200124

circles with normal vectors w_1, \ldots, w_k in the counterclockwise orientation. $A(Q_{i,j})$, $A(Q_{i,j,k})$ and $A(w_1, \ldots, w_k)$ denote the area of $Q_{i,j}$, the area of $Q_{i,j,k}$ and the area of (w_1, \ldots, w_k) , respectively.

Definition A.4. We denote by $T_{i,j}$, the quadrilateral in 3-space that is formed by joining the vertices of the edge e_i with the vertices of the edge e_j . The normal vectors of $T_{i,j}$, denoted n_1 , n_2 , n_3 , n_4 , are normal vectors to the great circles that bound $Q_{i,j}$ and are determined by the algorithm described in §2ai when i < j. We define the spherical faces of the quadrangles from the quadrilateral as follows: at each vertex of the quadrilateral extend each edge by length 1 and connect those segments that share a common vertex by an arc on the unit sphere (see figure 7 for an illustrative example). We call the spherical faces at the vertex i and i + 1, (corresponding to the vectors n_1 , n_3), the left and right faces of $T_{i,j}$ and the spherical faces at j and j + 1 (corresponding to n_2 and n_4), the top and bottom faces. One pair bounds $Q_{i,j}$ and the other bounds $Q_{i,j}^A$, but the reflections of these spherical faces through the centre of the sphere create both quadrangles.

Definition A.5. We will say that $T_{i,j}$ generates the quadrangle that contains the pair of right and left spherical faces of $T_{i,j}$ (the spherical faces at i and i+1, respectively). We call the antipodal quadrilateral of $T_{i,j}$, we denote $T_{i,j}^A$, the quadrilateral which generates $Q_{i,j}^A$. We denote its normal vectors as \mathbf{n}_1^A , \mathbf{n}_2^A , \mathbf{n}_3^A , \mathbf{n}_4^A

Remark A.6. We note that in a quadrangle generated by a quadrilateral $T_{i,j}$ the vectors either point inward or outward the quadrangle and their numbering either follows a counterclockwise or clockwise orientation on $Q_{i,j}$, depending on the sign of $\epsilon_{i,j}$. If the normal vectors of $Q_{i,j}$ point inwards (outwards resp.) than those of $Q_{i,j}^A$ point outwards (inwards resp.) and with the opposite numbering sequence (clockwise/counterclockwise).

Lemma A.7. Let $T_{i,j}$ denote the quadrilateral formed by e_i , e_j with vertices at the points p_i , p_{i+1} , p_j , p_{j+1} . The antipodal of $T_{i,j}$, $T_{i,j}^A$ is the tetrahedral formed by the edge e_i and the edge e_j^A , with vertices $p_{j^A} = p_{i+1} - (p_j - p_i)$ and $p_{(j+1)^A} = p_{i+1} - (p_{j+1} - p_i)$.

Proof. Let n_1 , n_2 , n_3 , n_4 denote the normal vectors to the faces of $T_{i,j}$ and let n_1^A , n_2^A , n_3^A , n_4^A denote the normal vectors of $T_{i,j}^A$. Without loss of generality, suppose that n_1 , n_2 , n_3 , n_4 all point inwards $Q_{i,j}$, numbered with the counterclockwise orientation. Then the antipodal, $Q_{i,j}^A$ has the same normal vectors but point outwards numbered with the clockwise orientation. The left and the right faces of $Q_{i,j}$ have normal vectors n_1 and n_3 . Since $Q_{i,j}^A$ is a reflection of $Q_{i,j}$ through the centre of the sphere, the normal vectors to $Q_{i,j}^A$ must be related to the normal vectors of $Q_{i,j}$ as follows: $n_1^A = -n_3$, $n_2^A = -n_2$, $n_3^A = -n_1$, $n_4^A = -n_4$.

We will examine if the normal vectors defined by $T_{i,j}^A$ satisfy these relations. Note that by definition

$$n_1^A = \frac{r_{i,j^A} \times r_{i,(j+1)^A}}{\|r_{ij^A} \times r_{i,(j+1)^A}\|},$$

where $r_{ij^A} = p_i - p_j^A = p_i - p_{i+1} + (p_j - p_i) = p_j - p_{i+1} = -r_{i+1,j}$, $r_{i,(j+1)^A} = p_i - p_{j+1}^A = p_i - p_{i+1} + (p_{j+1} - p_i) = p_{j+1} - p_i = -r_{i,j+1}$. Thus, $n_1^A = -n_3$.

Similarly, one can verify that the normal vectors of $T_{i,j}^A$, n_1^A , n_2^A , n_3^A , n_4^A satisfy: $n_1^A = -n_3$, $n_2^A = -n_2$, $n_3^A = -n_1$ and $n_4^A = -n_4$.

The following theorem determines the probability that three edges, two of which are consecutive, cross in a projection direction.

Theorem A.8. Let e_i , e_j , e_{j+1} denote three edges in 3-space. Then the joint probability of crossing between the projections of e_i , e_j and e_i , e_{j+1} , is equal to $(1/2\pi)A(Q_{i,j,j+1})$, where $Q_{i,j,j+1}$ is given in tables 1 and 2.

Proof. Let $T_{i,j}$ and $T_{i,j+1}$ be the two quadrilaterals formed by e_i , e_j and e_i , e_{j+1} , where e_i connects vertex i to i+1, e_j connect vertex j to j+1 and vertex j+1 to j+2. Let n_1 , n_2 , n_3 , n_4 denote

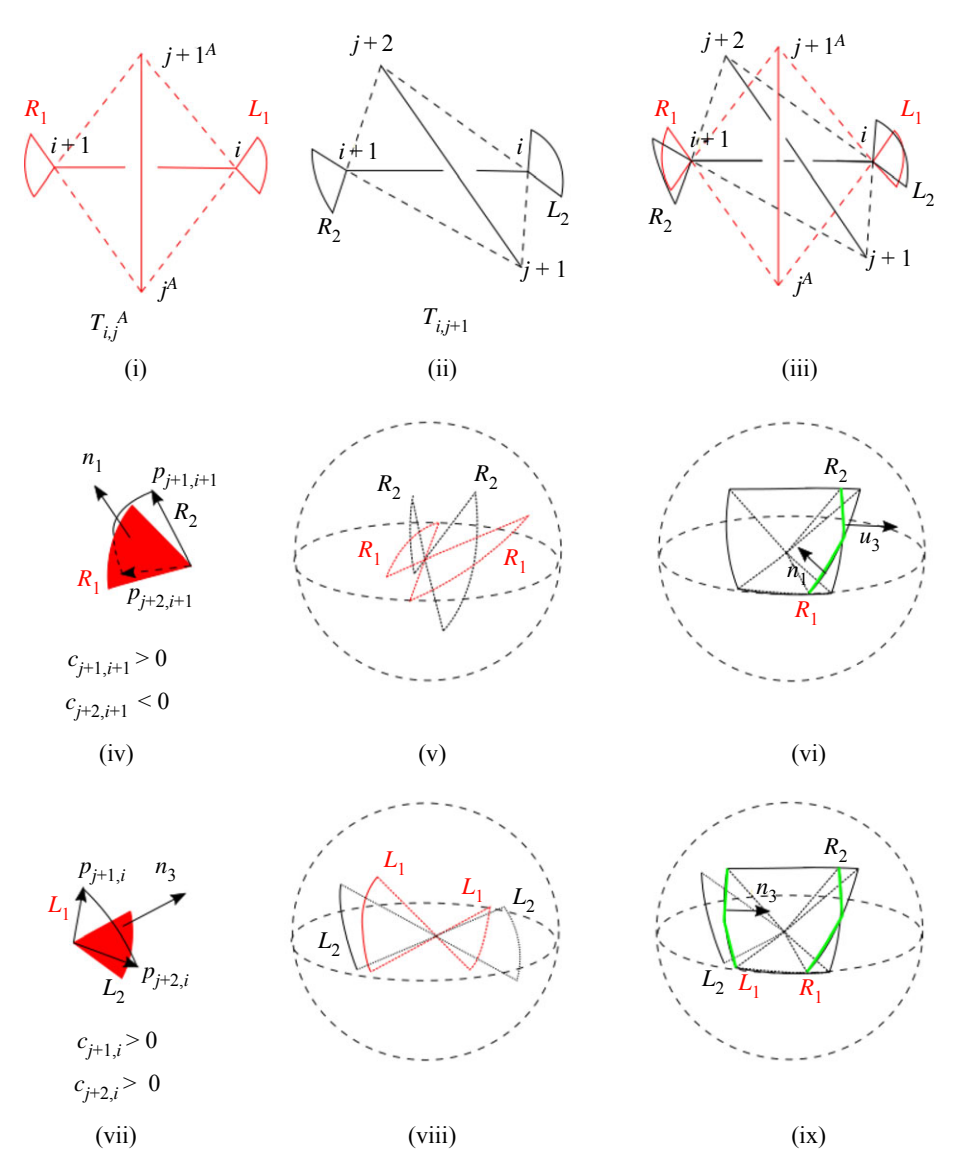


Figure 7. The quadrangle $Q_{i,j,j+1} = (Q_{i,j} \cap Q_{i,j+1}) \cup (Q_{i,j}^A \cap Q_{i,j+1})$ contains the vectors that define projections of e_i, e_j and e_i, e_{j+1} where the projections of both pairs intersect. This figure shows the procedure for determining $Q_{i,j}^A \cap Q_{i,j+1}$ in the case where $\epsilon_{i,j} = \epsilon_{i,j+1}$. $Q_{i,j}^A \cap Q_{i,j+1}$ is bounded by the great circles defined by the intersection of the faces of the quadrilaterals $T_{i,j}^A$ and $T_{i,j+1}$. (i) The quadrilateral $T_{i,j}^A$, (ii) the quadrilateral $T_{i,j+1}^A$, (iii) the relative positions of $T_{i,j}^A$ and $T_{i,j+1}$. (iv–ix) At the vertices i, i+1, we can define the left and right spherical faces of $Q_{i,j}^A$ and $Q_{i,j+1}$. To find the left and right faces of $Q_{i,j}^A \cap Q_{i,j+1}$, we examine the intersection of the spherical faces at i and at i+1 (see definition A.4). Let $p_{j+1,j+1}, p_{j+2,j+1}$ be the vectors that connect vertex j+1 and vertex j+2 to j+1. In this example, $c_{j+1,j+1} = (p_{j+1,j+1} \cdot n_1)\epsilon_{i,j} > 0$ and $c_{j+2,j+1} = (p_{j+2,j+1} \cdot n_3)\epsilon_{i,j} < 0$ and the spherical faces R_1, R_2 intersect and they both bound Q_1 . Similarly, in this example, $c_{j+1,j} = p_{j+1,j} \cdot n_3 > 0$ and $c_{j+2,j} = p_{j+2,j} \cdot n_3 > 0$ and only the spherical face L_1 bounds $Q_{i,j}^A \cap Q_{i,j+1}$. (Online version in colour.)

the normal vectors to the faces of $T_{i,j}$ and u_1 , u_2 , u_3 , u_4 denote the normal vectors to the faces of $T_{i,j+1}$. The normal vectors defined by the quadrilaterals define great circles which intersect to form the corresponding quadrangles. Each pair of great circles intersects at two antipodal points on the sphere, but due to the connectivity of the edges, there are also points where more than two

Table 1. The spherical polygon $Q_{i,j,j+1}$ in the case where the signs satisfy $\epsilon_{i,j} = \epsilon_{i,j+1}$, depending on the conformation. The spherical polygon $Q_{i,j,j+1}$ contains the vectors which define planes where the projections of e_i, e_j and e_i, e_{j+1} both cross. (w_1, w_2, \ldots, w_n) denotes the spherical polygon bounded by the great circles with normal vectors $w_i, i = 1, \ldots, n$, in the counterclockwise orientation (see definition A.3 and proof of theorem A.8).

$\epsilon_{ij} = \epsilon_{i,j+1}$, $w < 0$, $w_0 < 0$	$Q_{i,j,j+1}$
$c_{j+1,i+1} > 0$, $c_{j+2,i+1} > 0$, $c_{j+1,i} > 0$, $c_{j+2,i} > 0$	$(n_4, n_1, -u_2, n_3)$
$c_{j+1,i+1} > 0$, $c_{j+2,i+1} > 0$, $c_{j+1,i} < 0$, $c_{j+2,i} < 0$	$(n_4, n_1, -u_2, -u_1)$
$c_{j+1,i+1} > 0$, $c_{j+2,i+1} > 0$, $c_{j+1,i} > 0$, $c_{j+2,i} < 0$	$(n_4, n_1, -u_2, -u_1, n_3)$
$c_{j+1,i+1} > 0$, $c_{j+2,i+1} > 0$, $c_{j+1,i} < 0$, $c_{j+2,i} > 0$	$(n_4, n_1, -u_2, n_3, -u_1)$
$c_{j+1,i+1} < 0, c_{j+2,i+1} < 0, c_{j+1,i} > 0, c_{j+2,i} > 0$	$(n_4, -u_3, -u_2, n_3)$
$c_{j+1,i+1} < 0, c_{j+2,i+1} < 0, c_{j+1,i} < 0, c_{j+2,i} < 0$	$(n_4, -u_3, -u_2, -u_1)$
$c_{j+1,i+1} < 0, c_{j+2,i+1} < 0, c_{j+1,i} > 0, c_{j+2,i} < 0$	$(n_4, -u_3, -u_2, -u_1, n_3)$
$c_{j+1,i+1} < 0, c_{j+2,i+1} < 0, c_{j+1,i} < 0, c_{j+2,i} > 0$	$(n_4, -u_3, -u_2, n_3, -u_1)$
$c_{j+1,i+1} > 0, c_{j+2,i+1} < 0, c_{j+1,i} > 0, c_{j+2,i} > 0$	$(n_4, n_1, -u_3, -u_2, n_3)$
$c_{j+1,i+1} > 0, c_{j+2,i+1} < 0, c_{j+1,i} < 0, c_{j+2,i} < 0$	$(n_4, n_1, -u_3, -u_2, -u_1)$
$c_{j+1,i+1} > 0$, $c_{j+2,i+1} < 0$, $c_{j+1,i} > 0$, $c_{j+2,i} < 0$	$(n_4, n_1, -u_3, -u_2, -u_1, n_3)$
$c_{j+1,i+1} > 0, c_{j+2,i+1} < 0, c_{j+1,i} < 0, c_{j+2,i} > 0$	$(n_4, n_1, -u_3, -u_2, n_3, -u_1)$
$c_{j+1,i+1} < 0, c_{j+2,i+1} > 0, c_{j+1,i} > 0, c_{j+2,i} > 0$	$(n_4, -u_3, n_1, -u_2, n_3)$
$c_{j+1,i+1} < 0, c_{j+2,i+1} > 0, c_{j+1,i} < 0, c_{j+2,i} < 0$	$(n_4, -u_3, n_1, -u_2, -u_1)$
$c_{j+1,i+1} < 0, c_{j+2,i+1} > 0, c_{j+1,i} > 0, c_{j+2,i} < 0$	$(n_4, -u_3, n_1, -u_2, -u_1, n_3)$
$c_{j+1,i+1} < 0, c_{j+2,i+1} > 0, c_{j+1,i} < 0, c_{j+2,i} > 0$	$(n_4-u_3,n_1,-u_2,n_3,-u_1)$
$\epsilon_{ij}=\epsilon_{i,j+1}$, $w>0$ or $w_0>0$	$Q_{i,j,j+1}$
	Ø

Table 2. The spherical polygon $Q_{i,j,j+1}$ in the case where the signs satisfy $\epsilon_{i,j} = -\epsilon_{i,j+1}$, depending on the conformation (see caption of table 1 for notation).

$\epsilon_{i,j} = -\epsilon_{i,j+1}, w < 0$	$Q_{i,j,j+1}$	$\epsilon_{i,j} = -\epsilon_{i,j+1}, w > 0$	$Q_{i,j,j+1}$
$c_{j+2,i} > 0, c_{j+2,i+1} > 0$	$(n_2, -u_1, -u_2, -u_3)$	$c_{j+2,i} > 0, c_{j+2,i+1} > 0$	$(n_2, -u_1, n_4, -u_3)$
$c_{j+2,i}<0$, $c_{j+2,i+1}<0$	$(n_2, n_1, -u_2, n_3)$	$c_{j+2,i}<0$, $c_{j+2,i+1}<0$	(n_2, n_1, n_4, n_3)
$c_{j+2,i}<0,c_{j+2,i+1}>0$	$(n_2, n_1, -u_2, -u_3)$	$c_{j+2,i}<0,c_{j+2,i+1}>0$	$(n_2, n_1, n_4, -u_3)$
$c_{j+2,i} > 0, c_{j+2,i+1} < 0$	$(n_2, -u_1, -u_2, n_3)$	$c_{j+2,i} > 0$, $c_{j+2,i+1} < 0$	$(n_2, -u_1, n_4, n_3)$

great circles cross. These great circles correspond to faces of the tetrahedrals that share a common edge. The great circles with normal vectors n_2 , n_4 , u_2 share the common edge i, i+1, n_1, n_2, u_1 share i, j+1 and n_2 , n_3 , u_3 share i+1, j+1. Due to the connectivity of the edges e_j , e_{j+1} , $T_{i,j}$ and $T_{i,j+1}$ share a common face, the one formed by the vertices i, i+1, j+1, which implies that the normal vectors n_2 and n_3 are collinear. Thus, the great circles n_3 and n_3 are a common face, which implies that either n_3 and n_3 are n_3 and $n_$

Suppose $\epsilon_{i,j} = \epsilon_{i,j+1}$ (see figure 8 for an illustrative example). Then in order for the projections of e_i, e_j, e_{j+1} to intersect, e_i must pierce the triangle defined by e_j, e_{j+1} . To check this, we examine the signs of $w_0 = (v_3 \times (-n_1)) \cdot (v_3 \times n_3)$ and $w = (u_2 \times (-n_2)) \cdot (u_2 \times n_4)$, where $v_3 = p_{i,j+2} \times p_{j+1,j+2}$. If $w_0 > 0$, then $Q_{i,j,j+1} = \emptyset$. The faces with normal vectors u_2, n_2, n_4 share a common edge and, if

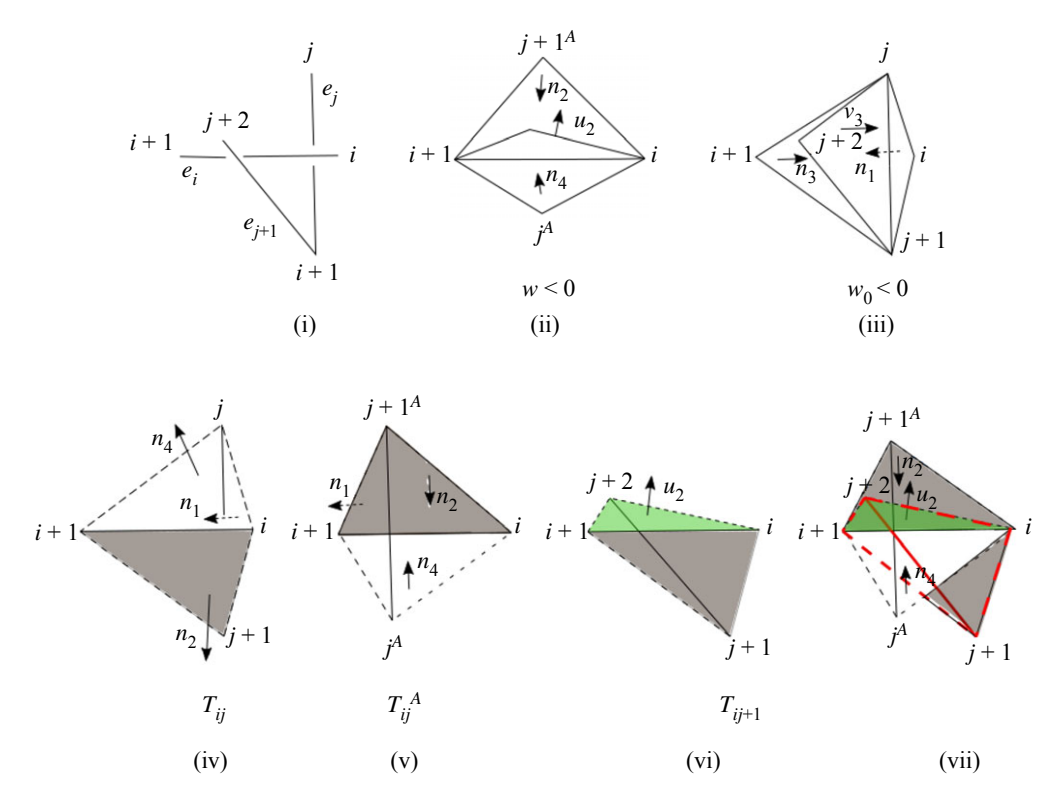


Figure 8. (i–iii) A configuration where $\epsilon_{ij} = \epsilon_{ij+1}$, w < 0 and $w_0 < 0$. (iv) The tetrahedral formed by e_i , e_j , we denote T_{ij} . (v) The antipodal of T_{ij} , we denote T_{ij}^A (see definition A.3 and theorem A.7). (vi) The tetrahedral formed by e_i , e_{j+1} . In this case, $T_{ij} \cap T_{ij+1} = \emptyset$. If $w = (u_2 \times (-n_2)) \cdot (u_2 \times n_4) > 0$, then $T_{ij}^A \cap T_{ij+1} = \emptyset$ as well, giving $A(Q_{ij,j+1}) = 0$. (vii) If w < 0, then $T_{ij}^A \cap T_{ij+1} \neq \emptyset$, giving $A(Q_{ij,j+1}) \neq 0$ (see proof of theorem A.8). (Online version in colour.)

 $(u_2 \times (-n_2)) \cdot (u_2 \times n_4) > 0$, then both n_2 and n_4 do not intersect $T_{i,j+1}$, so $A(Q_{i,j,j+1}) = 0$ (figure 8). Suppose that $w_0 < 0$ and w < 0. In that case $n_2 = -u_4$ and the face i, i+1, j contains the only points in the intersection of $T_{i,j}$ with $T_{i,j+1}$, thus $A(Q_{i,j} \cap Q_{i,j+1}) = 0$. We, therefore, examine the intersection of $T_{i,j}^A \cap T_{i,j+1}$, which determines $Q_{i,j}^A \cap Q_{i,j+1}$ (see theorem A.7). Since $n_2^A = -n_2 = u_4$, and $T_{i,j}^A$ is the antipodal of $T_{i,j}$, the face of $T_{i,j}^A$ with normal vector n_2^A and the face of $T_{i,j+1}$ with normal vector u_4 lie in the same plane but do not intersect (as shown in figure 8). Since w < 0 we know that $A(Q_{i,j,j+1}) \neq 0$ and it is formed by u_2, n_4 and, at least some of, the vectors u_1, u_3, n_1, n_3 .

To find the other faces of $Q_{i,j,j+1}$, we think at the level of right and left spherical faces of the tetrahedra $T_{i,j}^A$ and $T_{i,j+1}$. These faces share a common vertex, the vertex i and i+1, respectively. The spherical face of $T_{i,j}^A$ (resp. $T_{i,j+1}$) at i has normal vector \mathbf{n}_1^A (resp. \mathbf{n}_1) and the spherical face of $T_{i,j}^A$ (resp. $T_{i,j+1}$) at i+1 has normal vector \mathbf{n}_3^A (resp. \mathbf{n}_3). We compare the direction of the edges $\mathbf{p}_{i,j+1}$, $\mathbf{p}_{i,j+2}$ at the vertex i with the direction of \mathbf{n}_1^A to determine the position of the spherical face that they define (the one with normal vector \mathbf{n}_1^A to determine the position of the spherical face that they define (the one with normal vector \mathbf{n}_1^A Taking into account that $\mathbf{n}_1^A = -\mathbf{n}_3$ and $\mathbf{n}_3^A = -\mathbf{n}_1$, and whether these vectors point inwards or outwards $Q_{i,j,j+1}$, depending on the sign of ϵ_{ij} , we let $c_{j+1,i+1} = (p_{j+1,i+1} \cdot n_1)\epsilon_{ij}$, $c_{j+2,i+1} = (p_{j+2,i} \cdot n_3)\epsilon_{ij}$, $c_{j+2,i} = (p_{j+2,i} \cdot n_3)\epsilon_{ij}$ (see figure 7 for an illustrative example) and we think as follows: If $c_{j+1,i+1} \cdot c_{j+2,i+1} > 0$, then only one of the great circles with normal vectors \mathbf{n}_1 , \mathbf{n}_2 will be on the boundary of $Q_{i,j,j+1}$ and if $c_{j+1,i+1} \cdot c_{j+2,i+1} < 0$, the spherical faces intersect and both bound $Q_{i,j,j+1}$. Namely, if $c_{j+1,i+1} > 0$ and $c_{j+2,i+1} > 0$, only \mathbf{n}_1 and not \mathbf{n}_2 are in the boundary of $Q_{i,j,j+1}$, if $c_{j+1,i+1} < 0$, then only \mathbf{n}_3 and not \mathbf{n}_1 is the boundary of $Q_{i,j,j+1}$. If $c_{j+1,i+1} > 0$ and $c_{j+2,i+1} < 0$, then only \mathbf{n}_3 and not \mathbf{n}_1 is the boundary of $Q_{i,j,j+1}$. If $c_{j+1,i+1} > 0$ and

Figure 9. (i) A configuration where $\epsilon_{ij}=-\epsilon_{ij+1}$. (ii) In this configuration w>0. (iii) The tetrahedral formed by e_i,e_j , T_{ij} (iv) The tetrahedral formed by e_i , e_{j+1} , $T_{i,j+1}$. (v) In this case, $T_{i,j}^A \cap T_{i,j+1} = \emptyset$ and $T_{i,j} \cap T_{i,j+1} \neq \emptyset$. If $w = (u_2 \times (-n_2))$. $(u_2 \times n_4) < 0$, then two faces of $Q_{i,i,i+1}$ have normal vectors n_2 , u_2 , otherwise, it is n_2 , n_4 (see proof of theorem A.8).

 $c_{i+2,i+1} < 0$ then both n_1 , u_3 are in the boundary of $Q_{i,j,k}$ in the following counterclockwise order n_4 , n_1 , $-u_3$, $-u_2$. If $c_{j+1,j+1} < 0$ and $c_{j+2,j+1} > 0$ then both u_3 , u_1 are in the boundary of $Q_{i,j,j+1}$ in the following counterclockwise order n_4 , $-u_3$, n_1 , $-u_2$.

In a similar way, we find which of the spherical edges formed by $T_{i,j+1}$, $T_{i,j}^A$ at the vertex i form the other side of the boundary of $Q_{i,j,j+1}$. We note that in this case, if $c_{j+1,i} > 0$, $c_{j+2,i} > 0$, then only n_3 is in the boundary of $Q_{i,j+1}$, if $c_{j+1,i} > 0$, $c_{j+2,i} < 0$, n_3 , u_1 both are in the following order counterclockwise $-u_2$, $-u_1$, n_3 , n_4 . If $c_{i+1,i} < 0$, $c_{i+2,i} > 0$, they both are but in the following order $-u_2$, n_3 , $-u_1$, n_4 . If $c_{j+1,i} < 0$, $c_{j+2,i} < 0$, only u_1 is in the boundary of $Q_{i,j,j+1}$ (figure 7).

Suppose that $\epsilon_{i,j} = -\epsilon_{i,j+1}$, then $A(Q_{i,j}^A \cap Q_{i,j+1}) = 0$ and $A(Q_{i,j,j+1}) = A(Q_{i,j} \cap Q_{i,j+1}) \neq 0$ for all values of w and one face of $Q_{i,j,j+1}$ has normal vector n_2 (see figure 9 for an illustrative example). If w < 0 the other face is u_2 and if $w \ge 0$, it is n_4 . The left and right faces are of both quadrilaterals share a common edge (the extension of the edges j + 1, i and j + 1, i + 1) and thus do not intersect. So, only one of each will be the boundary of $Q_{i,j,j+1}$. To determine which, we check if $c_{j+2,i}$ $(p_{j+2,i} \cdot n_1)\epsilon_{ij} > 0$, then u_1 is the boundary, otherwise it is n_1 . If $c_{j+2,i+1} = (p_{j+2,i} \cdot n_3)\epsilon_{ij} > 0$, then u_3 is the boundary, otherwise it is n_3 .

Downloaded from https://royalsocietypublishing.org/ on 17 April 202

Theorem A.9. Let E_4 denote a polygonal curve of 4 edges in 3 space. The probability that its projection on a random projection direction is the non-trivial knotoid k2.1 is equal to

$$p_{k2.1}^{(4)} = p_{k2.1_{Bi}}^{(4)} + p_{k2.1_{Bii}}^{(4)}$$
(A 1)

where $k2.1_{Bi}$ and $k2.1_{Bii}$ are the two possible k2.1 diagrams (see case B(i) and case B(ii) in figure 6), $p_{k2.1}^{(4)} =$ $P(K((E_4)_{\xi}) = k2.1), p_{k2.1_{Bi}}^{(4)} = P((E_4)_{\xi} = k2.1_{Bi}), p_{k2.1_{Bii}}^{(4)} = P((E_4)_{\xi} = k2.1_{Bii})$ and where

$$p_{k2.1_{Bi}}^{(4)} = \begin{cases} 0, & \text{if } \epsilon_{1,3} \neq \epsilon_{1,4} \text{ or } w > 0 \text{ or } w_0 > 0 \\ \frac{1}{2\pi} \operatorname{Area}(v_3, -v_2, -u_2) & \text{if } c_{4,1} < 0, w < 0, w_0 < 0 \\ \frac{1}{2\pi} \operatorname{Area}(v_3, -v_2, n_1, -u_2) & \text{if } c_{4,1} > 0, w < 0, w_0 < 0, \end{cases}$$
(A 2)

where $c_{4,1} = (p_{4,1} \cdot n_1)\epsilon_{1,3}$, $w = (u_2 \times (-n_2)) \cdot (u_2 \times n_4)$, $w_0 = (v_3 \times (-n_1)) \cdot (v_3 \times n_3)$ and the vectors u_2 , n_2 , n_4 , v_3 , v_2 and n_1 are normal to the planes containing the vertices 014, 013, 021, 243, 241 and 023, respectively. $p_{k2.1_{Bii}}^{(4)} = p_{k2.1_{Bii}}^{'(4)}$ where $p_{k2.1_{Bii}}^{'(4)} = P((R(E_4))_{\xi} = k2.1_{Bi})$ and where $R(E_4)$ is the walk E_4 with reversed orientation.

Proof. Using the notation of proposition A.1, the probability of having a non-trivial knotoid in a random projection is equal to the probability of case B (i) or (ii) shown in figure 6 with crossings $\epsilon_{1,3} = \epsilon_{1,4}$. By proposition A.2 if one of the two is non-zero the other is zero. Thus, it suffices to find the probability that a projection of a polygonal curve of 4 edges is of the form case B (i) with

royalsocietypublishing.org/journal/rspa *Proc. R. Soc. A* **476**: 20200124

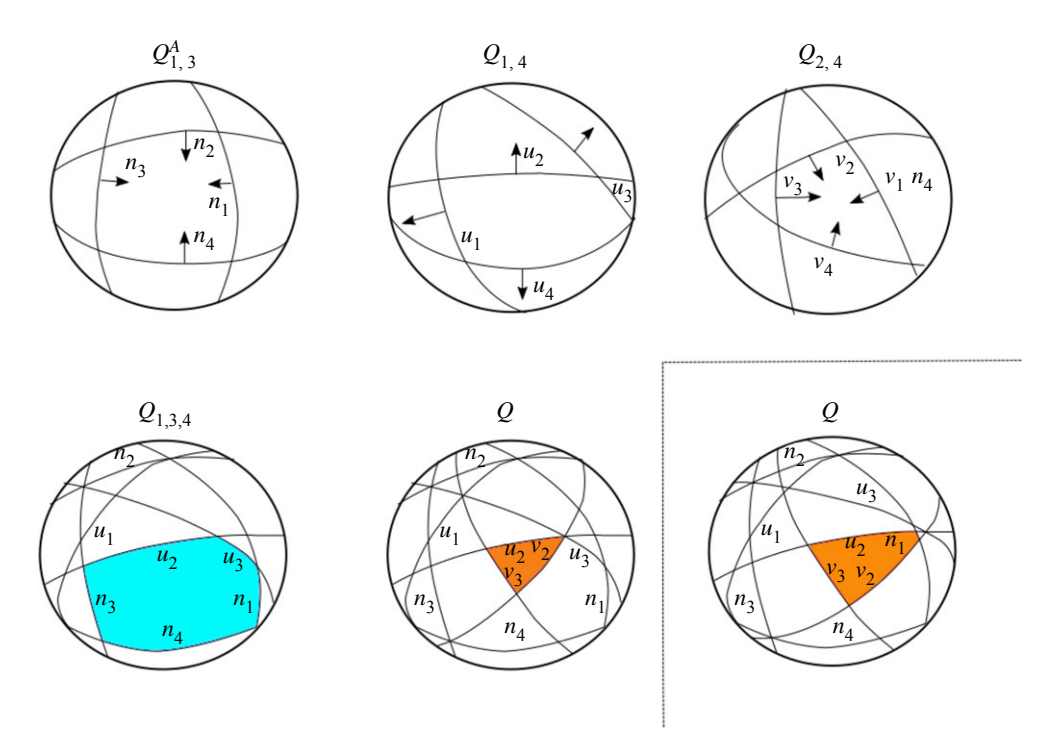


Figure 10. The spherical quadrangles $Q_{1,3}^A$, $Q_{1,4}$ and $Q_{2,4}$ defined by the faces of the quadrilaterals of the configuration shown in figure 8(i), with i = 1, j + 2. $Q_{1,3,4} = Q_{1,3} \cap Q_{1,4}$ contains the vectors which define projections of e_1, e_3, e_4 where both pairs e_1 , e_3 and e_1 , e_4 cross. Q is those vectors which define projections where the projection of the curve gives the knotoid k2.1(configuration case B(i) from figure 6). Depending on the positions of the great circles, the resulting Q could be that shown in the margin. (Online version in colour.)

 $\epsilon_{1,3} = \epsilon_{1,4}$, and if that probability is equal to 0, then one needs to compute the probability that it is of the type case B (ii) with $\epsilon_{1,4} = \epsilon_{2,4}$. To find a closed formula for these cases, it suffices to find a closed formula for the probability that it is non-trivial case B (i), since the same formula applied to the polygonal curve with reversed orientation of edges, will give the probability of getting case B (ii), $\epsilon_{1.4} = \epsilon_{2.4}$.

Let $\epsilon_{i,j,\xi}$ denote the sign of the crossing between the projections of the edges e_i, e_j to the plane with normal vector $\boldsymbol{\xi}$. This variable takes the values $\epsilon_{i,j,\boldsymbol{\xi}} = \epsilon_{i,j}$ when the projections of e_i,e_j cross in the plane with normal vector ξ and $\epsilon_{i,j,\xi} = 0$ when the projections of e_i, e_j do not cross in that plane.

The condition for $(E_4)_{\xi}$ being case B (i) with $\epsilon_{1,3} = \epsilon_{1,4}$ is: $\epsilon_{1,3,\xi} = \epsilon_{1,4,\xi} \neq 0$, $\epsilon_{2,4,\xi} = 0$ and $(e_4)_{\xi}$ lies in the side of $(e_3)_{\xi}$ that is inside the k2.1 bounded region. Without loss of generality, let us focus in the case of $\epsilon_{1,3,\xi} = \epsilon_{1,4,\xi} = 1$. Let us denote these conditions as: $(\epsilon_{1,3,\xi} = 1) \cap (\epsilon_{1,4,\xi} = 1) \cap (\epsilon_{2,4,\xi}) = 1$ $0 \cap C_{e_4,e_3}$, where C_{e_4,e_3} denotes the condition on $(e_4)_{\xi}$ being in the side of $(e_3)_{\xi}$ that is inside the region bounded by the projection of the edges e_1 , e_2 , e_3 . Thus

$$p_{k2.1}^{(4)} = \frac{A(Q_{1,3,4} \cap ((S^2 \setminus Q_{2,4}) \cap C_{e_4,e_3})}{2\pi},$$
(A 3)

where we cancelled a factor 2 in the numerator which arises because antipodal vectors give the

Since $\epsilon_{1,3} = \epsilon_{1,4}$, $Q_{1,3,4} = Q_{1,3}^A \cap Q_{1,4}$ (see theorem A.8 for i = 1, j = 3). The quadrangles $Q_{1,3}^A$, $Q_{1,4}$ and $Q_{2,4}$ are generated by the quadrilaterals $T_{1,3}^A$, $T_{1,4}$ and $T_{2,4}$ (figure 10). The normal vectors of $T_{1,3}^A$ are $n_1^A = -n_3$, $n_2^A = -n_2$, $n_3^A = -n_1$, $n_4^A = -n_4$, which define the faces of the quadrilateral in a counterclockwise order, all pointing outward $Q_{1,3}^A$. The normal vectors of $T_{1,4}$ are u_1, u_2, u_3, u_4 , where $u_2 = -u_4$, and all point outward $Q_{1,4}$ and the normal vectors of $T_{2,4}$ are v_1, v_2, v_3, v_4 in counterclockwise order, where $u_3 = v_4, u_3 = -v_1$, and they all point inward $Q_{2,4}$ (figure 10). So, in total we have nine vectors, which define nine great circles on S^2 .

 $Q_{1,3,4}$ was computed in theorem A.8. $Q_{1,3,4}$ is formed by n_4 , u_2 and some of n_3 , u_3 , n_1 , u_1 . To find $Q_{1,3,4} \cap ((S^2 \setminus Q_{2,4}) \cap C_{e_4,e_3})$, we think as follows: First, we note that if $Q_{1,3,4} \neq \emptyset$, then $Q_{2,4} \subset Q_{1,4}$. This quadrangle will include great circles defined by the normal vectors v_i (that involve the edges e_4 , e_2). Note that the great circles with normal vectors v_2 , u_4 and u_3 intersect (bottom left corner of Q_{134} , see figure 10) and the great circles with normal vectors v_2 , u_2 and u_3 also intersect (top right corner of Q_{134}). Thus, v_2 intersects the interior of $Q_{1,3,4}$. Since v_2 bounds $Q_{2,4}$ and points inwards $Q_{2,4}$, in order to be in $S^2 \setminus Q_{2,4}$, we need the part of $Q_{1,3,4}$ in the hemisphere defined by v_2 in the direction $-v_2$. The crossing of u_1 and u_3 must occur outside of $Q_{1,4}$ and $Q_{1,4}^A$ Thus, their crossing will occur in $Q_{1,3} \setminus Q_{1,3,4}$. Similarly, the crossing of n_1 , n_3 will cross inside $Q_{1,4} \setminus Q_{1,3,4}$. v_3 goes through both of these crossing points thus v_3 intersects the interior of $Q_{1,3,4}$. To be in the region C_{e_4,e_3} (in order to avoid projections of the form B_i'), we are interested in the hemisphere defined by the great circle with normal vector v_3 in the direction of v_3 . Taking all this into account, Q_1 will be either equal to $(v_3, -v_2, n_1, -u_2)$ or to $(-v_2, -u_2, v_3)$, depending on whether the crossing of v_2 with v_2 occurs inside or outside $Q_{1,3,4}$. Thus, we have shown that, if $Q \neq 0$, then $A(Q) = A(v_3, -v_2, n_1, -u_2)$, if $C_{4,1} = (p_4, \cdot n_1) \in I_4$, $C_{4,1} = (p_4, \cdot n_1) \in I_$

If $Q = \emptyset$, then we check for case B(ii), by repeating the same algorithm for the walk with reversed orientation.

Corollary A.10. Let E_4 denote a polygonal curve of 4 edges, e_1 , e_2 , e_3 , e_4 in 3-space, then the normalized bracket polynomial of E_4 is

$$f(E_4) = p_{k2,1}^{(4)}((-A)^3)^{-2\epsilon_{2,4}}\langle k2.1\rangle + (1 - p_{k2,1}^{(4)}), \tag{A4}$$

where $p_{k2,1}^{(4)}$ is defined in theorem A.9.

References

Downloaded from https://royalsocietypublishing.org/ on 17 April 2021

- 1. Arsuaga J, Vazquez M, McGuirk P, Trigueros S, Sumners DW, Roca J. 2005 DNA knots reveal a chiral organization of DNA in phage capsids. *Proc. Natl Acad. Sci. USA* **102**, 9165–9169. (doi:10.1073/pnas.0409323102)
- 2. Liu Y, O'Keeffe M, Treacy M, Yaghi O. 2018 The geometry of periodic knots, polycatenanes and weaving from a chemical perspective: a library for reticular chemistry. *Chem. Soc. Rev.* 47, 4642–4664. (doi:10.1039/C7CS00695K)
- 3. Panagiotou E, Millett KC, Atzberger PJ. 2019 Topological methods for polymeric materials: characterizing the relationship between polymer entanglement and viscoelasticity. *Polymers* 11, 11030437. (doi:10.3390/polym11030437)
- 4. Qin J, Milner ST. 2011 Counting polymer knots to find the entanglement length. *Soft Matter* **7**, 10 676–10 693. (doi:10.1039/c1sm05972f)
- 5. Ricca R. 2008 Topology bounds energy of knots and links. *Proc. R. Soc. A* **464**, 293–300. (doi:10.1098/rspa.2007.0174)
- Sulkowska JI, Rawdon EJ, Millett KC, Onuchic JN, Stasiak A. 2012 Conservation of complex knotting and slipknotting in patterns in proteins. *Proc. Natl Acad. Sci. USA* 109, E1715–E1723. (doi:10.1073/pnas.1205918109)
- 7. Edwards SF. 1967 Statistical mechanics with topological constraints: I. *Proc. Phys. Soc.* **91**, 513–519. (doi:10.1088/0370-1328/91/3/301)
- 8. Kauffman LH. 1991 *Knots and physics*, vol. 1. Series on Knots and Everything. Singapore: World Scientific.
- 9. Freyd P, Yetter D, Hoste J, Lickorish W, Millett KC, Ocneanu A. 1985 A new polynomial invariant for knots and links. *Bull. Am. Math. Soc.* 12, 239–246. (doi:10.1090/S0273-0979-1985-15361-3)
- 10. Jones VFR. 1985 A polynomial invariant of knots via von Neumann algebras. *Bull. Am. Math. Soc.* **12**, 103–112. (doi:10.1090/S0273-0979-1985-15304-2)

- 11. Jones VFR. 1987 Hecke algebra representations of braid groups and link polynomials. *Ann. Math.* 126, 335–388. (doi:10.2307/1971403)
- 12. Kauffman LH. 1987 State models and the Jones polynomial. *Topology* **26**, 395–407. (doi:10.1016/0040-9383(87)90009-7)
- 13. Kauffman LH. 1990 An invariant of regular isotopy. *Trans. Am. Math. Soc.* **318**, 417–471. (doi:10.1090/S0002-9947-1990-0958895-7)
- 14. Przytycki J, Traczyk P. 1987 Conway algebras and skein equivalence of links. *Proc. Am. Math. Soc.* **100**, 744–48. (doi:10.1090/S0002-9939-1987-0894448-2)
- 15. Gauss KF. 1877 Werke. Göttingen, Germany: Kgl. Gesellsch. Wiss.
- Gügümcu N, Kauffman LH. 2017 New invariants of knotoids. Eur. J. Comb. 65, 186–229. (doi:10.1016/j.ejc.2017.06.004)
- 17. Gügümcu N, Kauffman LH. 2019 Parity in knotoids. (http://arxiv.org/abs/1905.04089), pp. 1–19.
- 18. Gügümcu N, Lambropoulou S. 2017 Knotoids, braidoids and applications. *Symmetry* **9**, 315. (doi:10.3390/sym9120315)
- 19. Turaev V. 2012 Knotoids. Osaka J. Math. 49, 195-223.

Downloaded from https://royalsocietypublishing.org/ on 17 April 202

- 20. Baiesi M, Orlandini E, Seno F, Trovato A. 2017 Exploring the correlation between the folding rates of proteins and the entanglement of their native state. *J. Phys. A: Math. Theor.* **50**, 504001. (doi:10.1088/1751-8121/aa97e7)
- 21. Panagiotou E. 2015 The linking number in systems with periodic boundary conditions. *J. Comput. Phys.* **300**, 533–573. (doi:10.1016/j.jcp.2015.07.058)
- 22. Panagiotou E, Kröger M. 2014 Pulling-force-induced elongation and alignment effects on entanglement and knotting characteristics of linear polymers in a melt. *Phys. Rev. E* **90**, 042602. (doi:10.1103/PhysRevE.90.042602)
- 23. Panagiotou E, Kröger M, Millett KC. 2013 Writhe and mutual entanglement combine to give the entanglement length. *Phys. Rev. E* **88**, 062604. (doi:10.1103/PhysRevE.88.062604)
- 24. Rogen P, Fain B. 2003 Automatic classification of protein structure by using Gauss integrals. *Proc. Natl Acad. Sci. USA* **100**, 119–124. (doi:10.1073/pnas.2636460100)
- 25. Goundaroulis D, Dorier J, Stasiak A. 2017 Studies of global and local entanglements of individual protein chains using the concept of knotoids. *Sci. Rep.* 7, 6309. (doi:10.1038/s41598-017-06649-3)
- Goundaroulis D, Gügümcu N, Lambropoulou S, Dorier J, Stasiak A, Kauffman LH. 2017 Topological methods for open-knotted protein chains using the concepts of knotoids and bonded knotoids. *Polymers* 9, 444. (doi:10.3390/polym9090444)
- 27. Banchoff T. 1976 Self-linking numbers of space polygons. *Indiana Univ. Math. J.* **25**, 1171–1188. (doi:10.1512/iumj.1976.25.25093)
- 28. Klenin K, Langówski J. 2000 Computation of writhe in modelling of supercoiled DNA. *Biopolymers* **54**, 307–17. (doi:10.1002/1097-0282(20001015)54:5<307::AID-BIP20>3.0.CO;2-Y)
- 29. Calvo JA. 2001 The embedding space of hexagonal knots. *Topol. Appl.* **112**, 137–174. (doi:10.1016/S0166-8641(99)00229-1)
- 30. Laso M, Karayiannis NC, Foteinopoulou K, Mansfield L, Kröger M. 2009 Random packing of model polymers: local structure, topological hindrance and universal scaling. *Soft Matter* 5, 1762–1770. (doi:10.1039/b820264h)
- 31. Millett KC, Dobay A, Stasiak A. 2005 Linear random knots and their scaling behavior. *Macromolecules* **38**, 601–606. (doi:10.1021/ma048779a)
- 32. Panagiotou E, Tzoumanekas C, Lambropoulou S, Millett KC, Theodorou DN. 2011 A study of the entanglement in systems with periodic boundary conditions. *Progr. Theor. Phys. Suppl.* **191**, 172–181. (doi:10.1143/PTPS.191.172)
- 33. Tzoumanekas C, Theodorou DN. 2006 Topological analysis of linear polymer melts: a statistical approach. *Macromolecules* **39**, 4592–4604. (doi:10.1021/ma0607057)
- 34. Panagiotou E, Plaxco KW. 2020 A topological study of protein folding kinetics. *Topol. Biopolym., AMS Contemp. Math. Ser.* **76**, 223.
- 35. Charles N, Gazzola M, Mahadevan L. 2019 Topology, geometry, and mechanics of strongly stretched and twisted filaments: solenoids, plectonemes, and artificial muscle fibers. *Phys. Rev. Lett.* **123**, 208003. (doi:10.1103/PhysRevLett.123.208003)
- 36. Patil VP, Sandt JD, Kolle M, Dunkel J. 2020 Topological mechanics of knots and tangles. *Science* **367**, 71–75. (doi:10.1126/science.aaz0135)
- O'Donnol D, Stasiak A, Buck D. 2018 Two convergent pathways of DNA knotting in replicating DNA molecules as revealed by θ-curve analysis. *Nucleic Acids Res.* 46, 9181–9188. (doi:10.1093/nar/gky559)

Knot polynomials of open and closed curves - Supplementary Information

Eleni Panagiotou^{#,*} and Louis H. Kauffman[§]

*Department of Mathematics and SimCenter, University of Tennessee at Chattanooga, TN 37403, USA, <eleni-panagiotou@utc.edu>

§Department of Mathematics, Statistics and Computer Science University of Illinois at Chicago Chicago, IL 60607-7045, USA and Department of Mechanics and Mathematics Novosibirsk State University Novosibirsk Russia <kauffman@uic.edu>

1 A finite form for the bracket polynomial of a polygonal curve with 4 edges

In this section we show that an equivalent finite form of bracket polynomial exists, reducing the computation of the integral to a computation of a few dot and cross products between vectors and some arcsin evaluations. Here we provide a finite form of the bracket polynomial for a polygonal curve of 4 edges. This could lead to the creation of its finite form for more edges.

1.1 Closed curves

The first non-trivial bracket polynomial of a closed polygonal curve is that of a polygon of 4 edges, since a polygon of 3 edges is a triangle in 3-space and all projections give a diagram of no crossings except a set of measure zero which corresponds to irregular projections. Let P_4 denote a polygon of 4 edges, e_1, e_2, e_3, e_4 that connect the vertices (0, 1), (1, 2), (2, 3) and (3, 0), respectively. Let $\epsilon_{i,j}$ denote the sign of the crossing between the projections of the edges e_i, e_j when they cross. Notice that $\epsilon_{i,j}$ is independent of the projection direction and can take the values 1 and -1.

Proposition 1.1. The bracket polynomial of a polygon of 4 edges, e_1, e_2, e_3, e_4 , in 3-space, P_4 , is equal to:

$$\langle P_4 \rangle = 2|L(e_1, e_3)|(-A^{3\epsilon_{1,3}}) + 2|L(e_2, e_4)|(-A^{3\epsilon_{2,4}}) + (1 - ACN(P_4))$$
 (1)

where L denotes the Gauss linking integral and ACN denotes the average crossing number.

Proof. In any projection direction there are 3 possible diagrams that may occur as a projection of P_4 : a diagram with no crossing, or a crossing between the projections of e_1, e_3 or a crossing between the projections of e_2, e_4 . Notice that not both crossings at the same diagram are possible (the line defined by the projection of e_1 cuts the plane in two regions. Since the projection of e_3 intersects the projection of e_1 , the projections of the vertices 2 and 3 lie in different regions. Since e_2 joins vertex 1 with 2 and e_4 joins vertex 3 with 0, e_2, e_4 lie in different regions, thus they cannot cross.) In the case where there is no crossing, the bracket polynomial of that projection is equal to 1. When there is a crossing, the bracket polynomial is equal to $-A^{\pm 3}$, where the sign of the exponent is determined

by the sign of the crossing in the projection. Since the probability of e_2 , e_4 crossing is equal to $2|L(e_2, e_4)|$ and the probability of e_1 , e_3 crossing is $2|L(e_1, e_3)|$, then the bracket polynomial is

$$\langle P_4 \rangle = 2|L(e_1, e_3)|(-A^{3\epsilon_{1,3}}) + 2|L(e_2, e_4)|(-A^{3\epsilon_{2,4}}) + (1 - ACN(P_4))$$
 (2)

where we used the fact that $ACN(P_4) = 2|L(e_1, e_3)| + 2|L(e_2, e_4)|$. Notice that, due to the connectivity of the polygonal curve, $\epsilon_{1,3} = -\epsilon_{2,4}$, thus Eq. 2 could be expressed as

$$\langle P_4 \rangle = 2|L(e_1, e_3)|(-A^{3\epsilon_{1,3}}) + 2|L(e_2, e_4)|(-A^{-3\epsilon_{1,3}}) + (1 - ACN(P_4))$$

1.2 Open curves

In the case of a polygonal curve with 3 edges, we denote E_3 , the Kauffman bracket polynomial is always trivial, but the writhe of a diagram of a projection of E_3 can be 0 or ± 1 , depending on whether e_1, e_3 cross when projected in a direction $\vec{\xi}$.

Proposition 1.2. Let E_3 denote a polygonal curve of 3 edges, e_1, e_2, e_3 in 3-space, then the bracket polynomial of E_3 is

$$\langle E_3 \rangle = 2|L(e_1, e_3)|(-A^3)^{\epsilon_{13}} + (1 - 2|L(e_1, e_3)|)$$

where $\epsilon_{1,3}$ is the sign of $L(e_1, e_3)$

Proof. Consider a polygonal curve of 3 edges e_1, e_2, e_3 , (E_3) . Then in a projection of E_3 , $(E_3)_{\vec{\xi}}$, one either sees no crossings, so $\langle (E_3)_{\vec{\xi}} \rangle = 1$, or there is a crossing between e_1 and e_3 , in which case $\langle (E_3)_{\vec{\xi}} \rangle = -A^{\epsilon_{1,3}}$, thus

$$\langle E_3 \rangle = p_{k0,0}^{(3)} + p_{k0,\epsilon_{1,3}}^{(3)} (-A^3)^{\epsilon_{1,3}}$$

= $(1 - 2|L(e_1, e_3)|) + 2|L(e_1, e_3)|(-A^3)^{\epsilon_{1,3}}$

where
$$p_{k0,0}^{(3)} = P(K((E_3)_{\vec{\xi}}) = k0, wr((E_3)_{\vec{\xi}}) = 0)$$
 and $p_{k0,\epsilon_{1,3}}^{(3)} = P(K((E_3)_{\vec{\xi}}) = k0, wr((E_4)_{\vec{\xi}}) = \epsilon_{1,3}).$

Let E_4 be composed by 4 edges, e_1, e_2, e_3, e_4 , connecting the vertices (0, 1), (1, 2), (2, 3), (3, 4), respectively.

Let E_4 denote a polygonal curve of 4 edges. Then, by Propositions A.1 and A.2 (in main manuscript), the only non-trivial bracket polynomial is k2.1 and the writhe of the diagram is either 2 or -2. All the possible writhe values in a k0 (trivial knotoid) diagram of E_4 can be determined by inspection of all the possible diagrams of a polygonal curve of 4 edges, given in Proposition A.1. Let us denote these diagrams as $k0_{A_1}, k0_{A_2}, k0_{A_3}, k0_{B_i}, k0_{B_{ii}}, k0_{B_{ii}}, k0_{B_{ii}}, k0_C$. Let us denote by wr the writhe of a diagram. Then one can see that $wr(k0_{A_1}) = \pm 1, wr(k0_{A_2}) = \pm 1, wr(k0_{A_3}) = \pm 1, wr(k0_{B_{ii}}) = 0$ or $\pm 2, wr(k0_{B_{ii}}) =$

$$\langle E_4 \rangle = p_{k2.1}^{(4)} \langle k2.1 \rangle + \sum_{j=-2}^{2} p_{k0,j}^{(4)} (-A^3)^j$$
$$= p_{k2.1}^{(4)} (A^2 - A^{-4} + 1) + \sum_{j=-2}^{2} p_{k0,j}^{(4)} (-A^3)^j$$

where $p_{k2.1}^{(4)} = P(K((E_4)_{\vec{\xi}}) = k2.1)$ denotes the geometric probability that a projection of E_4 gives the non-trivial knotoid k2.1 (obtained in Theorem A.2 in main manuscript) and where $p_{k0,j}^{(4)} = P(K((E_4)_{\vec{\xi}}) = k0, wr((E_4)_{\vec{\xi}}) = j)$ denotes the probability of obtaining a diagram of the trivial knotoid with writhe j. The rest of this section is focused on obtaining finite forms for these probabilities.

Theorem 1.1. Let E_4 denote a polygonal curve of 4 edges, e_1, e_2, e_3, e_4 in 3-space, then the bracket polynomial of E_4 is

$$\langle E_4 \rangle = p_{k2.1}^{(4)} \langle k2.1 \rangle + p_{k0,\epsilon_{2,4}}^{(4)} (-A^3)^{\epsilon_{2,4}} + p_{k0,-\epsilon_{2,4}}^{(4)} (-A^3)^{-\epsilon_{2,4}} + p_{k0,-2\epsilon_{2,4}}^{(4)} (-A^3)^{-2\epsilon_{2,4}} + p_{k0,2\epsilon_{2,4}}^{(4)} (-A^3)^{2\epsilon_{2,4}} + p_{k0,0}^{(4)}$$

where the coefficients are:

$$p_{k2.1}^{(4)} = \begin{cases} \frac{1}{2\pi} A(Q), & \text{if } \epsilon_{1,3} = \epsilon_{1,4} \\ 0, & \text{otherwise} \end{cases}$$
 (3)

$$p_{k0,\epsilon_{2,4}}^{(4)} = \begin{cases} 2|L(e_{2},e_{4})| - \frac{1}{2\pi}A(Q_{4,2,1}), \epsilon_{1,3} = \epsilon_{1,4} \\ 2|L(e_{2},e_{4})| + 2|L(e_{1},e_{4})| - \frac{1}{2\pi}(A(Q_{4,2,1}) + A(Q_{2}) + A(Q_{1})), & \text{if } \epsilon_{2,4} = \epsilon_{1,4} = -\epsilon_{1,3} \\ 2|L(e_{2},e_{4})| + 2|L(e_{1},e_{3})| - \frac{1}{2\pi}(A(Q_{4,2,1}) + A(Q_{1})), & \text{if } \epsilon_{2,4} = \epsilon_{1,3} = -\epsilon_{1,4} \end{cases}$$

$$(4)$$

$$p_{k0,-\epsilon_{2,4}}^{(4)} = \begin{cases} 2|L(e_1,e_3)| + 2|L(e_1,e_4)| - \frac{1}{2\pi}(A(Q_{1,3,4}) + A(Q_2) + A(Q_1)), \epsilon_{1,3} = \epsilon_{1,4} \\ 2|L(e_1,e_3)| - \frac{1}{2\pi}A(Q_{1,3,4}), & \text{if } \epsilon_{2,4} = \epsilon_{1,4} = -\epsilon_{1,3} \\ 2|L(e_1,e_4)| - \frac{1}{2\pi}(A(Q_{1,3,4}) + A(Q_2)), & \text{if } \epsilon_{2,4} = \epsilon_{1,3} = -\epsilon_{1,4} \end{cases}$$

$$(5)$$

$$p_{k0,2\epsilon_{2,4}}^{(4)} = \begin{cases} \frac{1}{2\pi} (A(Q_2) - A(Q)), & \text{if } \epsilon_{2,4} = \epsilon_{1,4} = -\epsilon_{1,3} \\ 0, & \text{otherwise} \end{cases}$$
 (6)

$$p_{k0,-2\epsilon_{2,4}}^{(4)} = \begin{cases} \frac{1}{2\pi} (A(Q_1) - A(Q)), & \text{if } \epsilon_{1,4} = \epsilon_{1,3} = -\epsilon_{2,3} \\ 0, & \text{otherwise} \end{cases}$$
 (7)

and

$$p_{k0,0}^{(4)} = 1 - p_{k0,-2\epsilon_{2,4}}^{(4)} + p_{k0,2\epsilon_{2,4}}^{(4)} + p_{k0,-\epsilon_{2,4}}^{(4)} + p_{k0,\epsilon_{2,4}}^{(4)} + p_{k2,1,-\epsilon_{2,4}}^{(4)}$$

$$(8)$$

where $\epsilon_{i,j}$ denotes the sign of the linking number between $e_i, e_j, Q_1 = Q_{1,3,4} \setminus Q_{2,4}, Q_2 = Q_{4,2,1} \setminus Q_{1,3}$ and $Q = Q((E_4)_{\vec{\xi}} = k2.1)$. P(Q) is derived in Theorem A.2 (in main manuscript) and Q_1 is shown in Table 1. $Q_{4,2,1}, Q_2$ are derived with the same formulas for the reversed polygonal curve.

Proof. In the following, for simplicity, we will write $P(A_1)$ to express the probability $P(K((E_4)_{\vec{\xi}}) = k0_{A_1})$, etc.

By Proposition A.2 (in main manuscript), k2.1 is a possible knotoid diagram only when $\epsilon_{1,3} = \epsilon_{1,4}$, in which case, it also implies that $\epsilon_{2,4} = -\epsilon_{1,3}$. The probability of obtaining k2.1 is found in Theorem A.2 (in main manuscript).

Thus, we only need to examine the probabilities of obtaining the trivial knotoid with a given writhe. By inspection of the diagrams shown in Figure 6 (in main manuscript), we first notice the following:

$$p_{k0,\epsilon_{2,4}}^{(4)} = \begin{cases} P(A_2), & \text{if } \epsilon_{1,3} = \epsilon_{1,4} = -\epsilon_{2,4} \\ P(A_3) + P(A_2) + P(C), & \text{if } \epsilon_{2,4} = \epsilon_{1,4} = -\epsilon_{1,3} \\ P(A_1) + P(A_2) + P(C), & \text{if } \epsilon_{2,4} = \epsilon_{1,3} = -\epsilon_{1,4} \end{cases}$$
(9)

$$p_{k0,-\epsilon_{2,4}}^{(4)} = \begin{cases} P(A_1) + P(A_3) + P(C), & \text{if } \epsilon_{1,3} = \epsilon_{1,4} = -\epsilon_{2,4} \\ P(A_1), & \text{if } \epsilon_{2,4} = \epsilon_{1,4} = -\epsilon_{1,3} \\ P(A_3), & \text{if } \epsilon_{2,4} = \epsilon_{1,3} = -\epsilon_{1,4} \end{cases}$$
(10)

$$p_{k0,2\epsilon_{2,4}}^{(4)} = \begin{cases} P(B_{ii}) + P(B_{ii}\prime), & \text{if } \epsilon_{2,4} = \epsilon_{1,4} = -\epsilon_{1,3} \\ 0, & \text{otherwise} \end{cases}$$
 (11)

$$p_{k0,-2\epsilon_{2,4}}^{(4)} = \begin{cases} P(B_i) + P(B_{i'}), & \text{if } \epsilon_{1,3} = -\epsilon_{1,4} = -\epsilon_{2,4} \\ 0, & \text{otherwise} \end{cases}$$
 (12)

We will compute these probabilities in the three cases: $\epsilon_{1,3} = \epsilon_{1,4}$, $\epsilon_{1,3} = -\epsilon_{1,4} = \epsilon_{2,4}$, $\epsilon_{1,3} = -\epsilon_{1,4} = -\epsilon_{2,4}$.

First, we notice that, in all cases, due to the connectivity of the polygonal curve,

$\epsilon_{1,3} = \epsilon_{1,4}, \ w < 0, w_0 < 0$	$Q_{1,3,4}$	Q_1
$c_{3,1} > 0, c_{4,1} > 0, c_{3,0} > 0, c_{4,0} > 0$	$(\vec{n}_4,\vec{n}_1,-\vec{u}_2,\vec{n}_3)$	$(\vec{n}_4, -\vec{v}_3, -\vec{u}_2, \vec{n}_3) \cup Q$
$c_{3,1} > 0, c_{4,1} > 0, c_{3,0} < 0, c_{4,0} < 0$	$(\vec{n}_4, \vec{n}_1, -\vec{u}_2, -\vec{u}_1)$	$(\vec{n}_4, -\vec{v}_3, -\vec{u}_2, -\vec{u}_1) \cup Q$
$c_{3,1} > 0, c_{4,1} > 0, c_{3,0} > 0, c_{4,0} < 0$	$(\vec{n}_4, \vec{n}_1, -\vec{u}_2, -\vec{u}_1, \vec{n}_3)$	$(\vec{n}_4, -\vec{v}_3, -\vec{u}_2, -\vec{u}_1, \vec{n}_3) \cup Q$
$c_{3,1} > 0, c_{4,1} > 0, c_{3,0} < 0, c_{4,0} > 0$	$(\vec{n}_4, \vec{n}_1, -\vec{u}_2, \vec{n}_3, -\vec{u}_1)$	$(\vec{n}_4, -\vec{v}_3, -\vec{u}_2, \vec{n}_3, -\vec{u}_1) \cup Q)$
$c_{3,1} < 0, c_{4,1} < 0, c_{3,0} > 0, c_{4,0} > 0$	$(\vec{n}_4, -\vec{u}_3, -\vec{u}_2, \vec{n}_3)$	$(\vec{n}_4, -\vec{v}_3, -\vec{u}_2, \vec{n}_3) \cup Q$
$c_{3,1} < 0, c_{4,1} < 0, c_{3,0} < 0, c_{4,0} < 0$	$(\vec{n}_4, -\vec{u}_3, -\vec{u}_2, -\vec{u}_1)$	$(\vec{n}_4, -\vec{v}_3, -\vec{u}_2, -\vec{u}_1) \cup Q$
$c_{3,1} < 0, c_{4,1} < 0, c_{3,0} > 0, c_{4,0} < 0$	$(\vec{n}_4, -\vec{u}_3, -\vec{u}_2, -\vec{u}_1, \vec{n}_3)$	$(\vec{n}_4, -\vec{v}_3, -\vec{u}_2, -\vec{u}_1, \vec{n}_3) \cup Q$
$c_{3,1} < 0, c_{4,1} < 0, c_{3,0} < 0, c_{4,0} > 0$	$(\vec{n}_4, -\vec{u}_3, -\vec{u}_2, \vec{n}_3, -\vec{u}_1)$	$\left \begin{array}{cccc} (\vec{n}_4, -\vec{v}_3, -\vec{u}_2, \vec{n}_3, -\vec{u}_1) \cup Q \end{array} \right $
$c_{3,1} > 0, c_{4,1} < 0, c_{3,0} > 0, c_{4,0} > 0$	$(\vec{n}_4, \vec{n}_1, -\vec{u}_3, -\vec{u}_2, \vec{n}_3)$	$(\vec{n}_4,-\vec{v}_3,-\vec{u}_2,\vec{n}_3)\cup Q$
$c_{3,1} > 0, c_{4,1} < 0, c_{3,0} < 0, c_{4,0} < 0$	$(\vec{n}_4, \vec{n}_1, -\vec{u}_3, -\vec{u}_2, -\vec{u}_1)$	$(\vec{n}_4, -\vec{v}_3, -\vec{u}_2, -\vec{u}_1) \cup Q$
$c_{3,1} > 0, c_{4,1} < 0, c_{3,0} > 0, c_{4,0} < 0$	$(\vec{n}_4, \vec{n}_1, -\vec{u}_3, -\vec{u}_2, -\vec{u}_1, \vec{n}_3)$	$(\vec{n}_4, -\vec{v}_3, -\vec{u}_2, -\vec{u}_1, \vec{n}_3) \cup Q$
$c_{3,1} > 0, c_{4,1} < 0, c_{3,0} < 0, c_{4,0} > 0$	$(\vec{n}_4, \vec{n}_1, -\vec{u}_3, -\vec{u}_2, \vec{n}_3, -\vec{u}_1)$	$(\vec{n}_4, -\vec{v}_3, -\vec{u}_2, \vec{n}_3, -\vec{u}_1) \cup Q$
$c_{3,1} < 0, c_{4,1} > 0, c_{3,0} > 0, c_{4,0} > 0$	$(ec{n}_4, -ec{u}_3, ec{n}_1, -ec{u}_2, ec{n}_3)$	$(\vec{n}_4, -\vec{v}_3, -\vec{u}_2, \vec{n}_3) \cup Q$
$c_{3,1} < 0, c_{4,1} > 0, c_{3,0} < 0, c_{4,0} < 0$	$(ec{n}_4, -ec{u}_3, ec{n}_1, -ec{u}_2, -ec{u}_1)$	$(\vec{n}_4, -\vec{v}_3, -\vec{u}_2, -\vec{u}_1) \cup Q$
$c_{3,1} < 0, c_{4,1} > 0, c_{3,0} > 0, c_{4,0} < 0$	$(\vec{n}_4,-\vec{u}_3,\vec{n}_1,-\vec{u}_2,-\vec{u}_1,\vec{n}_3)$	$(\vec{n}_4, -\vec{v}_3, -\vec{u}_2, -\vec{u}_1, \vec{n}_3) \cup Q$
$c_{3,1} < 0, c_{4,1} > 0, c_{3,0} < 0, c_{4,0} > 0$	$(\vec{n}_4, -\vec{u}_3, \vec{n}_1, -\vec{u}_2, \vec{n}_3, -\vec{u}_1)$	$(\vec{n}_4, -\vec{v}_3, -\vec{u}_2, \vec{n}_3, -\vec{u}_1) \cup Q$
$\epsilon_{1,3} = \epsilon_{1,4}, \ w > 0 \text{ or } w_0 > 0$	$Q_{1,3,4}$	Q_1
	Ø	Ø
$\epsilon_{1,3} = -\epsilon_{1,4}, w < 0$	$Q_{1,3,4}$	Q_1
$c_{4,0} > 0, c_{4,1} > 0$	$(\vec{n}_2, -\vec{u}_1, -\vec{u}_2, -\vec{u}_3)$	$Q_{1,3,4} \setminus (\vec{v}_1, \vec{v}_2, \vec{v}_3, \vec{n}_2)$
$c_{4,0} < 0, c_{4,1} < 0$	$(ec{n}_2,ec{n}_1,-ec{u}_2,ec{n}_3)$	$Q_{1,3,4}$
$c_{4,0} < 0, c_{4,1} > 0$	$(ec{n}_2,ec{n}_1,-ec{u}_2,-ec{u}_3)$	$Q_{1,3,4} \setminus (\vec{v}_1, \vec{v}_2, \vec{n}_1, \vec{n}_2)$
$c_{4,0} > 0, c_{4,1} < 0$	$(\vec{n}_2, -\vec{u}_1, -\vec{u}_2, \vec{n}_3)$	$Q_{1,3,4}$
$\epsilon_{1,3} = -\epsilon_{1,4}, w > 0$	$Q_{1,3,4}$	Q_1
$c_{4,0} > 0, c_{4,1} > 0$	$(\vec{n}_2, -\vec{u}_1, \vec{n}_4, -\vec{u}_3)$	$Q_{1,3,4} \setminus (-\vec{u}_3, \vec{n}_4, \vec{v}_3, \vec{n}_2)$
$c_{4,0} < 0, c_{4,1} < 0, c_{4\prime,1\prime} > 0$	$(ec{n}_2,ec{n}_1,ec{n}_4,ec{n}_3)$	$Q_{1,3,4} \setminus (\vec{v}_3, -\vec{v}_2, \vec{n}_2, \vec{n}_1, \vec{n}_4)$
$c_{4,0} < 0, c_{4,1} < 0, c_{4\prime,1\prime} < 0$	$(ec{n}_2,ec{n}_1,ec{n}_4,ec{n}_3)$	$Q_{1,3,4} \setminus (\vec{v}_3, -\vec{v}_2, \vec{n}_1, \vec{n}_4)$
$c_{4,0} < 0, c_{4,1} > 0$	$(\vec{n}_2, \vec{n}_1, \vec{n}_4, -\vec{u}_3)$	Ø
$c_{4,0} > 0, c_{4,1} < 0$	$(ec{n}_2, -ec{u}_1, ec{n}_4, ec{n}_3)$	$Q_{1,3,4}$

Table 1: The spherical polygons $Q_{1,3,4}$ and $Q_1 = Q_{1,3,4} \setminus Q_{2,4}$, respectively, are computed by using the above expressions. The expression $(\vec{w}_1, \dots, \vec{w}_n)$ denotes the spherical polygon defined by the intersection of the great circles with normal vectors $\vec{w}_1, \dots, \vec{w}_n$ in the counterclockwise orientation (see Definition A.1 in main manuscript). The expressions depend on the conformation of the curve in 3-space, where $c_{3,1} = (\vec{p}_{3,1} \cdot \vec{n}_1)_{\epsilon_{1,3}}$, $c_{4,1} = (\vec{p}_{4,1} \cdot \vec{n}_1)\epsilon_{1,3}$, $c_{3,0} = (\vec{p}_{3,0} \cdot \vec{n}_3)\epsilon_{1,3}$, $c_{4,0} = (\vec{p}_{4,0} \cdot \vec{n}_3)\epsilon_{1,3}$, $c_{4,1} = (\vec{p}_{1,4} \cdot (-\vec{v}_2))\epsilon_{2,4}$ and $w = (\vec{u}_2 \times (-\vec{n}_2)) \cdot (\vec{u}_2 \times \vec{n}_4)$, where $\vec{n}_1, \vec{u}_i, \vec{v}_i$ are the normal vectors to the quadrilaterals $T_{1,3}, T_{1,4}, T_{2,4}$ and where $\vec{p}_{i,j}$ is the vector that connects vertex i to vertex j in 3-space. The areas of $Q_{4,2,1}$ and Q_2 are obtained from the areas $Q_{1,3,4}$ and Q_1 of the polygonal curve with reversed orientation (see proof of Theorem 1.1).

$$Q_{2,4} \cap Q_{1,3} \subset Q_{2,4} \cap Q_{1,4} = Q_{4,2,1}$$

$$Q_{2,4} \cap Q_{1,3} \subset Q_1 = Q_{1,3} \cap Q_{1,4} = Q_{1,3,4}$$
(13)

The probabilities can be expressed as:

$$\begin{split} P(A_1) &= 2|L(e_1,e_3)| - \frac{1}{2\pi}A(Q_{1,3,4}) \\ P(A_2) &= 2|L(e_1,e_3)| - \frac{1}{2\pi}A(Q_{4,2,1}) \\ P(A_3) &= 2|L(e_1,e_4)| - \frac{1}{2\pi}A(Q_{4,2,1} \setminus Q_{1,3}) - A(Q_{1,3,4}) \\ P(C) &= \frac{1}{2\pi}A(Q_{2,4} \cap Q_{1,3,4}) \\ P(B_i) + P(B_{i'}) &= \frac{1}{2\pi}A(Q_{1,3,4} \setminus Q_{2,4}) \\ P(B_{ii}) + P(B_{ii'}) &= \frac{1}{2\pi}A(Q_{4,2,1} \setminus Q_{1,3}) \end{split}$$

From all these equations, and using the notation $Q_1 = Q_{1,3,4} \setminus Q_{2,4}$ and $Q_2 = Q_{4,2,1} \setminus Q_{1,3}$, we obtain the expressions of the statement of the Theorem.

We proceed with finding finite forms for $Q_{1,3,4}$ and Q_1 from which the finite forms of $Q_{4,2,1}$ and Q_2 are also derived.

Finite form of $Q_{1,3,4}$

The finite form of $Q_{1,3,4}$ is found by Theorem A.1 (in main manuscript) for i = 0, j = 2. Finite form of $Q_{4,2,1}$:

For the finite form of $Q_{4,2,1}$ we think as follows: Let $R(E_4)$ to denote the polygonal curve E_4 with reversed numbering of vertices. Let us denote its edges e'_1, e'_2, e'_3, e'_4 . Then $Q_{4,2,1} = Q_{1',3',4'}$. This can be obtained from table 1 determined by the algorithm described in Section 2(a)(i) for n_i' , u_i' which are related to the normal vectors of E_4 as follows: $\vec{n}_1' = -\vec{v}_2$, $\vec{n}_2' = -\vec{v}_1$, $\vec{n}_3' = -\vec{v}_4$, $\vec{n}_4' = -\vec{v}_3$, $\vec{u}_1' = -\vec{u}_2$, $\vec{u}_2' = -\vec{u}_1$, $\vec{u}_3' = -\vec{u}_4$, $\vec{u}_4' = -\vec{u}_3$. Accordingly, $w' = (\vec{u}_1 \times \vec{v}_1) \cdot (\vec{u}_1 \times (-\vec{v}_3))$, $w_0' = (\vec{n}_4 \times \vec{v}_2) \cdot (\vec{n}_4 \times \vec{n}_3)$, $\epsilon_{1',3'} = \epsilon_{2,4}$ and $\epsilon_{1',4'} = \epsilon_{1,4}$. Finally, $\epsilon_{3',1'} = (\vec{p}_{3',1'} \cdot \vec{n}_1')\epsilon_{1',3'} = (\vec{p}_{1,3} \cdot (-\vec{v}_2)\epsilon_{2,4}$, otherwise $\epsilon_{4',1'} = (\vec{p}_{4',1'} \cdot \vec{n}_1')\epsilon_{1',3'} = (\vec{p}_{1,4} \cdot (-\vec{v}_2))\epsilon_{2,4}$, $\epsilon_{3',0'} = (\vec{p}_{3',0'} \cdot \vec{n}_3')\epsilon_{1',3'} = (\vec{p}_{1,4} \cdot (-\vec{v}_4))\epsilon_{2,4}$, when $\epsilon_{1',3'} = \epsilon_{1',4'}$ and $\epsilon_{4',0'} = (\vec{p}_{4',0'} \cdot \vec{n}_1')\epsilon_{1',3'} = (\vec{p}_{0,4} \cdot (-\vec{v}_4))\epsilon_{2,4}$, when $\epsilon_{1',3'} = \epsilon_{1',4'}$ and $\epsilon_{4',0'} = (\vec{p}_{4',0'} \cdot \vec{n}_1')\epsilon_{1',3'} = (\vec{p}_{4',1'} \cdot \vec{n}_3')\epsilon_{1',3'} = (\vec{p}_{0,3} \cdot (-\vec{v}_4))\epsilon_{2,4}$, when $\epsilon_{1',3'} = -\epsilon_{1',4'}$ Finite form of Q_1

- Case $\epsilon_{1,4} = \epsilon_{1,3} = -\epsilon_{2,4}$: One can derive from the proof of Theorem A.2 (in main manuscript) the area of $Q_{1,3,4} \setminus Q_{2,4}$. The area will be $Q_1 = Q \cup (\vec{n}_4, -\vec{v}_3, -\vec{u}_2, x)$, where x is equal to $-\vec{u}_1$ or \vec{n}_3 or $\vec{n}_3, -\vec{u}_1$ or $-\vec{u}_1, \vec{n}_3$, depending on the signs of $c_{0,3}, c_{0,4}$ (see Table 1).

Next, we consider the case $\epsilon_{1,4} = -\epsilon_{1,3}$ and refer to Figure 1 as an illustrative example. Since $\vec{u}_3 = -\vec{v}_1$ and $\vec{n}_3 = \vec{v}_4$, these spherical edges (which bound $Q_{2,4}$) do not cross the interior of $Q_{1,3,4}$. In order to find $Q_1 = Q_{1,3,4} \setminus Q_{2,4}$, we examine if and how \vec{v}_2 and \vec{v}_3 intersect the interior of $Q_{1,3,4}$. Figure 1 shows the relative positions of $\vec{v}_1, \vec{v}_4, \vec{v}_2$ determined by the connectivity of the polygonal curve and the orientations of \vec{v}_1, \vec{v}_4 are also given by the known orientations of \vec{u}_3 and \vec{n}_3 .

- Case $\epsilon_{1,4} = -\epsilon_{1,3} = \epsilon_{2,4}$: (This is the case where $c_{4,1} < 0$ in Table 1). This corresponds to the case where $\epsilon_{1\prime,4\prime} = \epsilon_{1\prime,3\prime}$ for the reversed walk. First of all, in this case, we notice that when $c_{4,0} > 0$, then $w\prime > 0$ and, similarly, when w < 0 then $w_0\prime > 0$, thus in these cases $Q_{4,2,1} = \emptyset$, giving $Q_1 = Q_{1,3,4}$. Thus, the only case that might give $Q_{2,4} \cap Q_{1,3,4} \neq \emptyset$ is the case $w > 0, c_{4,0} < 0$, equivalently, $w > 0, w_0 < 0$, (see Figure 1). In that case the great circle with normal vector \vec{v}_3 intersects the interior of $Q_{1,3,4}$ (since the face with normal vector \vec{v}_3 is in-between the faces with normal vectors \vec{n}_1, \vec{n}_3). To examine the intersection of $Q_{2,4} \cap Q_{1,3,4}$, we examine the reversed oriented polygon, $R(E_4)$ (see previous paragraph). The above conditions correspond to the case where $\epsilon_{1\prime,3\prime} = \epsilon_{1\prime,4\prime}$, $w\prime < 0, w_0\prime < 0$, which is the case that can give the non-trivial knotoid. Thus, using Theorem ??, we derive that for $w\prime < 0$, if $c_{4\prime,1\prime} > 0$, then $Q_1 = Q_{1,3,4} \setminus (v_3, -v_2, n_1, n_4)$ and if $c_{4\prime,1\prime} < 0$, then $Q_1 = Q_{1,3,4} \setminus (v_3, -v_2, n_1, n_4)$.

- Case $\epsilon_{1,4} = -\epsilon_{1,3} = -\epsilon_{2,4}$: (This is the case where $c_{4,1} > 0$ in Table 1) As in the previous case, in order to find $Q_1 = Q_{1,3,4} \setminus Q_{2,4}$, we need the area of $Q_{1,3,4}$ that is determined by the great circles \vec{v}_2 and \vec{v}_3 . To find these intersections, we will examine $Q_{4,2,1}$ using the reverse walk with $\epsilon_{1\prime,3\prime} = -\epsilon_{1\prime,4\prime}$, and we notice that in all cases, $c_{1\prime,4\prime} = (p_{4\prime,1\prime} \cdot \vec{n}_3\prime)\epsilon_{1\prime,3\prime} = (p_{0,3} \cdot (-\vec{v}_4))\epsilon_{2,4} = (p_{0,3} \cdot (-\vec{n}_3))\epsilon_{1,3} > 0$. Indeed, since \vec{n}_3 is the normal vector to the face defined by the vertices 1,2,3, of the tetrhedral $T_{1,4}$ and points inwards if $\epsilon_{1,3} > 0$ (in the direction of vertex 3) or outwards otherwise. Thus $c_{1\prime,4\prime} > 0$ in all cases. Thus, the intersection will depend on the sign of $c_{0\prime,4\prime} = (p_{4\prime,0\prime} \cdot \vec{n}_1\prime)\epsilon_{1\prime,3\prime} = (p_{0,4} \cdot (-\vec{v}_2))\epsilon_{2,4}$. This sign will depend on the sign of $c_{4,0} = (\vec{p}_{4,0} \cdot \vec{n}_1)\epsilon_{1,3}$ and the sign of w, which determines if \vec{u}_2 lies between \vec{n}_2 , \vec{n}_4 .

If $c_{4,0} < 0$ then w' < 0 since we can verify that the face with normal vector \vec{u}_1 is between the faces with normal vectors \vec{v}_1, \vec{v}_3 , and w' > 0 if $c_{4,0} > 0$. If w < 0 then $c_{0\prime,4\prime} = (p_{4\prime,0\prime} \cdot \vec{n}_1\prime)\epsilon_{1\prime,3\prime} = (p_{0,4} \cdot (-\vec{v}_2))\epsilon_{2,4} < 0$ since \vec{v}_2 points in the opposite direction of the region that contains the vertex 0 when $\epsilon_{2,4} < 0$, and $c_{0\prime,4\prime} > 0$ if w > 0.

Thus, by using Table 1 for the reversed walk we find that if $c_{4,0} < 0$ and w < 0, then $Q_1 = Q_{1,3,4} \setminus (v_1, v_2, n_1, n_2)$. If $c_{4,0} < 0$ and w > 0, then $Q_1 = \emptyset$. If $c_{4,0} > 0$ and w < 0, then $Q_1 = Q_{1,3,4} \setminus (v_1, v_2, v_3, n_2)$. If $c_{4,0} > 0$ and w > 0, then $Q_1 = Q_{1,3,4} \setminus (v_1, n_4, v_3, n_2)$. Finite form of Q_2 :

For the finite form of Q_2 we think as follows: Let $R(E_4)$ to denote the polygonal curve E_4 with reversed numbering of vertices as described in the Finite form of $Q_{4,2,1}$. Then $Q_2 = Q_{4,2,1} \setminus Q_{1,3} = Q_{1',3',4'} \setminus Q_{2',4'} = Q_1'$, which is found earlier.

Example: (continuation of Example in main manuscript) Figure 2 shows the Kauffman bracket polynomial of the open 3-dimensional curve in time and that of the standard diagram of the knotoid k2.1. We see the bracket polynomial of the open curve vary continuously in time, tending to that of the diagram, due to the tightening of the configuration to become almost planar.

* Work supported by NSF DMS - 1913180

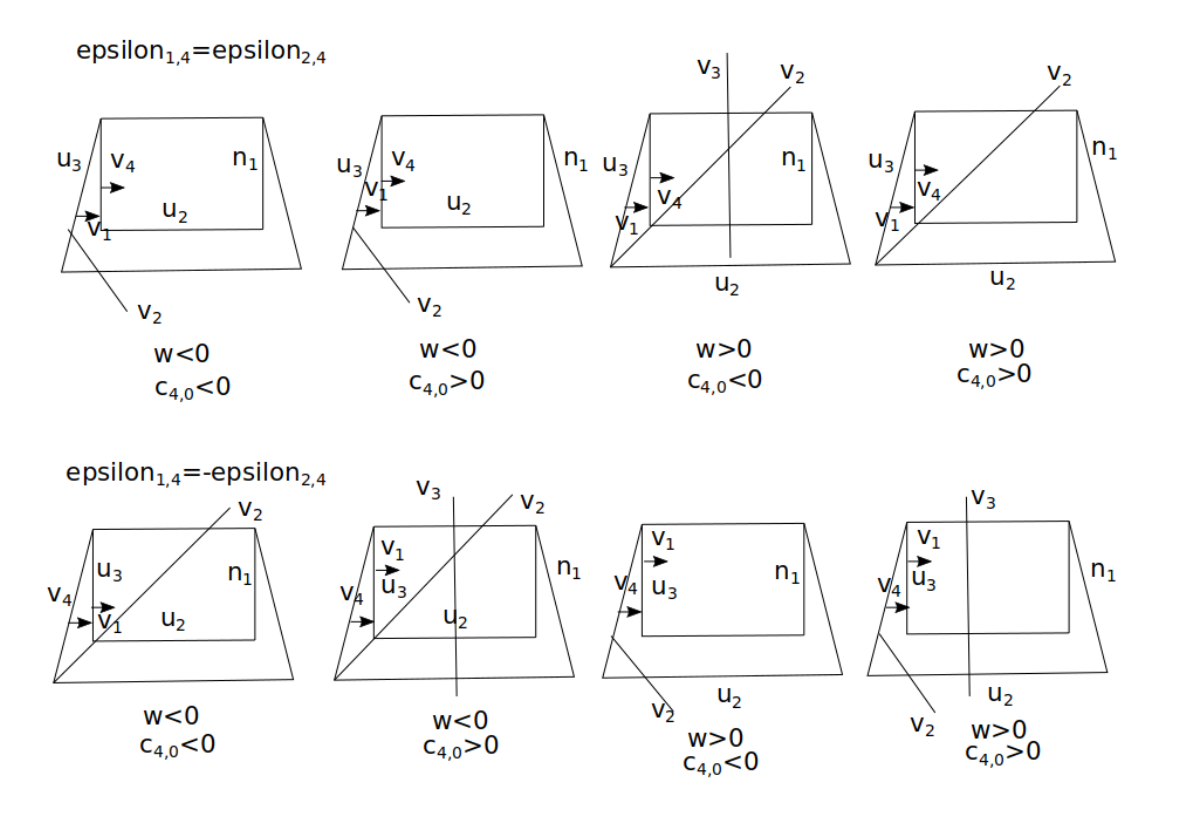


Figure 1: Representation of $Q_{1,3,4}$ when $\epsilon_{1,3} = \epsilon_{2,4}$. In this case, one great circle of the boundary of $Q_{1,3,4}$ is the one with normal vector \vec{n}_2 (top boundary in the figure). The lower great circle (bottom boundary) is \vec{u}_2 or \vec{n}_4 , depending on whether $\epsilon_{1,4} = \epsilon_{2,4}$ or not (equivalently, depending on the sign of $c_{1,4}$). Similar considerations define the other boundaries, where $c_{4,0} = (\vec{p}_{4,0} \cdot \vec{n}_1)\epsilon_{1,3}$, $w = (\vec{u}_2 \times (-\vec{n}_2)) \cdot (\vec{u}_2 \times \vec{n}_4)$, $\vec{n}_3 = \vec{v}_4$ and $\vec{u}_3 = -\vec{v}_1$. To determine $Q_1 = Q_{1,3,4} \setminus Q_{2,4}$, we examine how \vec{v}_2 and \vec{v}_3 intersect $Q_{1,3,4}$ (see proof of Theorem 1.1). The results are shown in Table 1.

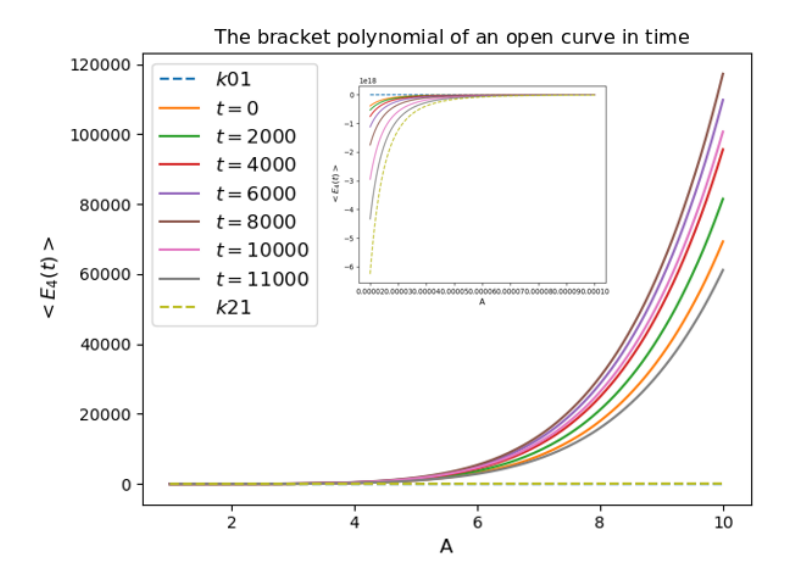


Figure 2: The Kauffman bracket polynomial of an open polygonal curve as it moves in time. The inset plot shows the polynomial for values of the parameter A less than 1.